
GLISp-r: A PREFERENCE-BASED OPTIMIZATION ALGORITHM WITH CONVERGENCE GUARANTEES

A PREPRINT

Davide Previtali

Department of Computer Science Engineering
University of Bergamo
davide.previtali@unibg.it

Mirko Mazzoleni

Department of Computer Science Engineering
University of Bergamo
mirko.mazzoleni@unibg.it

Antonio Ferramosca

Department of Computer Science Engineering
University of Bergamo
antonio.ferramosca@unibg.it

Fabio Previdi

Department of Computer Science Engineering
University of Bergamo
fabio.previdi@unibg.it

ABSTRACT

Preference-based optimization algorithms are iterative procedures that seek the optimal value for a decision variable based only on comparisons between couples of different samples. At each iteration, a human decision-maker is asked to express a preference between two samples, highlighting which one, if any, is better than the other. The optimization procedure must use the observed preferences to find the value of the decision variable that is most preferred by the human decision-maker, while also minimizing the number of comparisons. In this work, we propose GLISp-r, an extension of a recent preference-based optimization procedure called GLISp. The latter uses a Radial Basis Function surrogate to describe the tastes of the individual. Iteratively, GLISp proposes new samples to compare with the current best candidate by trading off exploitation of the surrogate model and exploration of the decision space. In GLISp-r, we propose a different criterion to use when looking for a new candidate sample that is inspired by MSRS, a popular procedure in the black-box optimization framework (which is closely related to the preference-based one). Compared to GLISp, GLISp-r is less likely to get stuck on local optimizers of the preference-based optimization problem. We motivate this claim theoretically, with a proof of convergence, and empirically, by comparing the performances of GLISp and GLISp-r on different benchmark optimization problems.

Keywords Global optimization, Preference-based optimization, Surrogate-based methods, Active preference learning.

1 Introduction

Preference-based optimization algorithms seek the global solution¹ of an optimization problem whose objective function is unknown and unmeasurable. The “goodness” of a certain *decision variable* is assessed by a human-decision maker, who is able to make comparisons between samples and state which of them he/she prefers. As pointed out in [3] (and referenced papers), it is best to let the individual compare only two samples at a time, instead of giving him/her multiple options, to avoid the “choice overload” effect and achieve a more reliable response.

In the context of complex control systems, often the performances associated to a regulator tuning might be evaluated by a human decision-maker whose judgment is expressed through visual inspection (or other sensory evaluations) of the behavior achieved by the system under control. Multiple experiments must be performed until the individual is satisfied by the closed-loop performances. If a trial and error approach is adopted, then there is no guarantee that the final tuning is optimal in some sense. Moreover, the calibration procedure might be quite time-consuming since

¹In general, an optimization problem can have multiple global solutions. Here, we consider the case where only one global solution is present. We do not make any assumptions on the local optimizers, which can be more than one.

possibly many combinations of the controller parameters need to be tested. A better alternative to the trial and error approach are preference-based optimization algorithms, which drive the experiments by proposing new values of the decision variable to try, using the preferences expressed by the individual. The goal is to seek the decision variable that is most preferred by the human decision-maker while also minimizing the number of comparisons (thus performing less experiments). Successful applications of preference-based optimization procedures include [35], where the authors use algorithm GLISp [3] to tune the controller for a continuous stirring tank reactor and for autonomous driving vehicles. The same algorithm has been employed in [27] to calibrate the parameters of a velocity planner for robotic tasks.

The preference-based optimization problem can be formalized by applying some *utility theory* concepts [24]. Suppose that there exists a preorder, called the *preference relation*, which describes the tastes of the individual (i.e. the outputs of the comparisons between couples of samples). If the preference relation associated to a human decision-maker is complete and continuous, then it is possible to *represent* it with a continuous (*latent*) *utility function* [8]. The latter is a function that assigns an abstract degree of “goodness” to all possible values of the decision variable. Moreover, the most preferred sample for a human decision-maker is the one that has the highest utility and corresponds to the optimizer of the preference-based optimization problem.

Most preference-based optimization algorithms rely on a *surrogate model*², which is an approximation of the latent utility function built from the preference information at hand. In general, any procedure that uses a surrogate model to solve an optimization problem is said to be a *surrogate-based* (or *surface response*) *method*. These algorithms are mostly used to solve *black-box optimization* problems, where the objective function is unknown but measurable (see [32, 18]), but they can also be employed to solve preference-based optimization problems, provided that the surrogate model is properly defined. In practice, preference-based surface response methods iteratively propose new samples to be compared with the current best candidate by properly trading-off *exploitation* (or local search), i.e. selecting samples that are likely to offer an improvement based on the current observations, and *exploration* (or global search), i.e. finding samples in regions of the domain of which we have little to no knowledge. Quite often, this is done by defining an *acquisition function*, which encapsulates these two aspects, and the next candidate sample is obtained by minimizing or maximizing it. Most surrogate models either rely on Gaussian Processes (GPs) [34], giving raise to (Preferential) Bayesian Optimization, or Radial Basis Functions (RBFs) [15]. For example, in [7] the authors propose a predictive model for the latent utility function based on GPs (preference learning task). The latter is used as a surrogate model in [6] to carry out preference-based optimization. Alternative Preferential Bayesian Optimization algorithms are proposed in [4] and in [13]. Recently, in [3], the authors developed a preference-based optimization method, called GLISp, that is based on a RBF approximation of the latent utility function.

In this work, we propose an *extension of the GLISp [3] algorithm*, that we will refer to as GLISp-r, which is more robust in finding the global solution of the preference-based optimization problem. To do so, we:

1. *Address some limitations of the exploration function* used in [3], which can cause the procedure to miss the global solution and get stuck on a local minima;
2. *Propose a dynamic trade-off between exploration and exploitation* (i.e. by allowing the “weight” of this two contributions to vary in between iterations). This is commonly done in the black-box optimization framework, see for example [15, 26, 33, 25], but it has not been tried for GLISp [3];
3. *Provide a proof of convergence* for GLISp-r, furtherly motivating its robustness. Currently, no such proof is present for GLISp [3].

This paper is organized as follows. In Section 2 we introduce the preference-based optimization problem from an utility theory perspective. Section 3 addresses how to build the surrogate model (as performed by GLISp [3]) and look for the next sample to evaluate, keeping in mind the exploration-exploitation trade-off. We also briefly cover the exploration function used in [3]. The latter is thoroughly analyzed in Section 4, where we propose a solution to the limitations that we have encountered in GLISp [3]. Section 5 describes algorithm GLISp-r and addresses its convergence. Then, Section 6 compares the performances of GLISp-r with GLISp [3] and C-GLISp [36], a revisitation of the latter method by the same authors, on some benchmark optimization problems. Section 7 gives some concluding remarks. Finally, Appendix A contains the proofs for some of the Theorems, Lemmas and Propositions that are given in this paper.

²For the sake of clarity, we want to make a clear distinction between *preference learning* and preference-based optimization. The former is tasked with actually estimating a predictive model, i.e., as it is common in machine learning problems, the objective is usually to approximate the latent utility function [12]. Instead, the latter aims to find the global optimizer of an optimization problem using only the information brought by the preferences. In practice, many preference-based optimization methods still use a predictive model as the surrogate model, yet its prediction accuracy is not the main concern.

2 Problem formulation

Consider the n -dimensional decision variable $\mathbf{x} = [x^{(1)} \ \dots \ x^{(n)}]^\top \in \mathbb{R}^n$ and suppose that we are interested in finding the sample that is most preferred by the human decision-maker within a subset of \mathbb{R}^n , namely $\Omega \subset \mathbb{R}^n$. We define the *constraint set* Ω as:

$$\Omega = \left\{ \mathbf{x} : \begin{array}{l} \mathbf{l} \leq \mathbf{x} \leq \mathbf{u}, \\ A_{ineq} \cdot \mathbf{x} \leq \mathbf{b}_{ineq}, \\ A_{eq} \cdot \mathbf{x} = \mathbf{b}_{eq}, \\ \mathbf{g}_{ineq}(\mathbf{x}) \leq \mathbf{0}_{p_{ineq}}, \\ \mathbf{g}_{eq}(\mathbf{x}) = \mathbf{0}_{p_{eq}} \end{array} \right\}. \quad \begin{array}{l} \text{bounds} \\ \text{linear inequalities} \\ \text{linear equalities} \\ \text{nonlinear inequalities} \\ \text{nonlinear equalities} \end{array} \quad (1)$$

In (1), $\mathbf{l}, \mathbf{u} \in \mathbb{R}^n$, $A_{ineq} \in \mathbb{R}^{q_{ineq} \times n}$, $\mathbf{b}_{ineq} \in \mathbb{R}^{q_{ineq}}$, $A_{eq} \in \mathbb{R}^{q_{eq} \times n}$, $\mathbf{b}_{eq} \in \mathbb{R}^{q_{eq}}$, $\mathbf{g}_{ineq} : \mathbb{R}^n \rightarrow \mathbb{R}^{p_{ineq}}$ and $\mathbf{g}_{eq} : \mathbb{R}^n \rightarrow \mathbb{R}^{p_{eq}}$. Notation-wise, $\mathbf{0}_{p_{ineq}}$ represents the p_{ineq} zero column vector (and similarly for $\mathbf{0}_{p_{eq}}$). We suppose that: (i) all of these constraints are completely known and (ii) Ω includes, at least, the bound constraints (the remaining equality and inequality constraints can be omitted).

In order to formalize the preference-based optimization problem, we review some *utility theory* [24] concepts. Consider the constraint set Ω in (1), we define a generic binary relation \mathcal{R} on Ω as a subset $\mathcal{R} \subseteq \Omega \times \Omega$. Notation-wise, given two samples $\mathbf{x}_i, \mathbf{x}_j \in \Omega$, we denote the ordered pairs for which the binary relation holds, $(\mathbf{x}_i, \mathbf{x}_j) \in \mathcal{R}$, as $\mathbf{x}_i \mathcal{R} \mathbf{x}_j$ [24].

A *preference relation*, $\succsim \subseteq \Omega \times \Omega$, is a preorder (a specific case of binary relation) which is commonly used to describe the tastes of an individual. In this context, $\mathbf{x}_i \succsim \mathbf{x}_j$ implies that a human decision-maker with preference relation \succsim deems sample \mathbf{x}_i at least as good as \mathbf{x}_j . The fact that the preference relation is a preorder encompasses the *rationality* of the individual, since the following properties hold:

1. *Reflexivity*, i.e. $\mathbf{x}_i \succsim \mathbf{x}_i, \forall \mathbf{x}_i \in \Omega$ (any alternative is as good as itself),
2. *Transitivity*, i.e. $\forall \mathbf{x}_i, \mathbf{x}_j, \mathbf{x}_k \in \Omega$, if $\mathbf{x}_i \succsim \mathbf{x}_j$ and $\mathbf{x}_j \succsim \mathbf{x}_k$ hold, then $\mathbf{x}_i \succsim \mathbf{x}_k$ (consistency of the preferences expressed by the individual).

Preference relation \succsim is usually “split” into two transitive binary relations:

- The *strict preference relation* \succ on Ω , i.e. $\mathbf{x}_i \succ \mathbf{x}_j$ if and only if $\mathbf{x}_i \succsim \mathbf{x}_j$ but not $\mathbf{x}_j \succsim \mathbf{x}_i$ (\mathbf{x}_i is “better than” \mathbf{x}_j), and
- The *indifference relation* \sim on Ω , i.e. $\mathbf{x}_i \sim \mathbf{x}_j$ if and only if $\mathbf{x}_i \succsim \mathbf{x}_j$ and $\mathbf{x}_j \succsim \mathbf{x}_i$ (\mathbf{x}_i is “as good as” \mathbf{x}_j).

Another common assumption on \succsim , which is not necessarily related to the rationality of the individual, is that it is a *complete* binary relation, i.e. either $\mathbf{x}_i \succsim \mathbf{x}_j$ or $\mathbf{x}_j \succsim \mathbf{x}_i$ hold $\forall \mathbf{x}_i, \mathbf{x}_j \in \Omega$. Completeness of \succsim implies that the human decision-maker is never uncertain, that is he/she is always able to express a preference between any couple of samples. One last relevant property for \succsim is *continuity*. Here, we avoid a formal definition of the continuity of a binary relation (see [24]) but, intuitively, if \succsim is continuous and $\mathbf{x}_i \succ \mathbf{x}_j$, then an alternative \mathbf{x}_k which is “very close” to \mathbf{x}_j should also be deemed strictly worse than \mathbf{x}_i by the individual.

Having defined the preference relation \succsim , we can state the goal of preference-based optimization, that is:

$$\text{find } \mathbf{x}^* \in \Omega \text{ such that } \mathbf{x}^* \succsim \mathbf{x}, \forall \mathbf{x} \in \Omega. \quad (2)$$

Formally, \mathbf{x}^* is called the \succsim -*maximum* of Ω , i.e. the sample that is most preferred by the human decision-maker. Concerning the existence of \mathbf{x}^* , we can state the following Proposition, which can be seen as a generalization of the Extreme Value Theorem [1] for preference relations.

Proposition 1 (Existence of a \succsim -maximum of Ω [24]). *A \succsim -maximum of Ω is guaranteed to exist if Ω is a compact subset of a metric space (in our case $\Omega \subset \mathbb{R}^n$) and \succsim is a continuous and complete preference relation on Ω .*

Proposition 1 will be relevant when proving the convergence of the proposed algorithm in Section 5. We can finally state one of the most important results in utility theory:

Theorem 1 (Debreu’s Utility Representation Theorem for \mathbb{R}^n [8]). *Let Ω be any nonempty subset of \mathbb{R}^n and \succsim be a complete preference relation on Ω . If \succsim is continuous, then it can be represented by a continuous utility function*

$u_{\succsim} : \Omega \rightarrow \mathbb{R}$ such that, $\forall \mathbf{x}_i, \mathbf{x}_j \in \Omega$:

$$\mathbf{x}_i \succsim \mathbf{x}_j \quad \text{if and only if} \quad u_{\succsim}(\mathbf{x}_i) \geq u_{\succsim}(\mathbf{x}_j).$$

Moreover, we have that:

$$\mathbf{x}_i \succ \mathbf{x}_j \quad \text{if and only if} \quad u_{\succsim}(\mathbf{x}_i) > u_{\succsim}(\mathbf{x}_j),$$

$$\mathbf{x}_i \sim \mathbf{x}_j \quad \text{if and only if} \quad u_{\succsim}(\mathbf{x}_i) = u_{\succsim}(\mathbf{x}_j).$$

Using Theorem 1, we can build an optimization problem to find the \succsim -maximum of Ω . In particular, in order to define a minimization problem as in [3], we define the *scoring function*, $f : \mathbb{R}^n \rightarrow \mathbb{R}$, as $f(\mathbf{x}) = -u_{\succsim}(\mathbf{x})$. Formally, $u_{\succsim}(\mathbf{x})$ and $f(\mathbf{x})$ have different domains (respectively, Ω and \mathbb{R}^n). However, assuming that $u_{\succsim}(\mathbf{x})$ is continuous and Ω is a compact subset of \mathbb{R}^n (which are either results or assumptions of Proposition 1 and Theorem 1), then there exists a continuous extensions of $u_{\succsim}(\mathbf{x})$ with domain \mathbb{R}^n (Tietze Extension Theorem [19]). Finally, we can re-write Problem (2) as:

$$\begin{aligned} \mathbf{x}^* &= \arg \min_{\mathbf{x}} f(\mathbf{x}) \\ \text{s.t.} \quad &\mathbf{x} \in \Omega. \end{aligned} \tag{3}$$

In GLISp [3], instead of considering the preference relation explicitly, the authors define the *preference function* $\pi : \mathbb{R}^n \times \mathbb{R}^n \rightarrow \{-1, 0, 1\}$ (which describes the output of the comparison between two samples) as:

$$\pi(\mathbf{x}_i, \mathbf{x}_j) = \begin{cases} -1 & \text{if } f(\mathbf{x}_i) < f(\mathbf{x}_j) \iff \text{if } \mathbf{x}_i \succ \mathbf{x}_j \\ 0 & \text{if } f(\mathbf{x}_i) = f(\mathbf{x}_j) \iff \text{if } \mathbf{x}_i \sim \mathbf{x}_j. \\ 1 & \text{if } f(\mathbf{x}_i) > f(\mathbf{x}_j) \iff \text{if } \mathbf{x}_j \succ \mathbf{x}_i \end{cases} \tag{4}$$

$\pi(\mathbf{x}_i, \mathbf{x}_j)$ is obtained from the utility representation of the binary relation \succsim (see Theorem 1) and from the fact that $f(\mathbf{x}) = -u_{\succsim}(\mathbf{x})$. Reflexivity and transitivity of the preorder \succsim are highlighted by the following properties of the preference relation:

1. $\pi(\mathbf{x}_i, \mathbf{x}_i) = 0, \forall \mathbf{x}_i \in \mathbb{R}^n$,
2. $\pi(\mathbf{x}_i, \mathbf{x}_j) = \pi(\mathbf{x}_j, \mathbf{x}_k) = b \Rightarrow \pi(\mathbf{x}_i, \mathbf{x}_k) = b, \forall \mathbf{x}_i, \mathbf{x}_j, \mathbf{x}_k \in \mathbb{R}^n$.

In the context of preference-based optimization, surrogate-based methods aim to solve Problem (3) starting from a set of N *distinct samples* of the decision variable \mathcal{X} :

$$\mathcal{X} = \{\mathbf{x}_i : i = 1, \dots, N, \mathbf{x}_i \in \Omega, \mathbf{x}_i \neq \mathbf{x}_j, \forall i \neq j\} \tag{5}$$

and a set of M *preferences* expressed by the human decision-maker:

$$\mathcal{B} = \{b_h : h = 1, \dots, M, b_h \in \{-1, 0, 1\}\}. \tag{6}$$

b_h is the h -th preference obtained by comparing a certain couple of samples, as highlighted by the following *mapping set*:

$$\begin{aligned} \mathcal{S} &= \left\{ (\ell(h), \kappa(h)) : h = 1, \dots, M, \ell(h), \kappa(h) \in \mathbb{N}, \right. \\ &\quad \left. b_h = \pi(\mathbf{x}_{\ell(h)}, \mathbf{x}_{\kappa(h)}), \right. \\ &\quad \left. b_h \in \mathcal{B}, \mathbf{x}_{\ell(h)}, \mathbf{x}_{\kappa(h)} \in \mathcal{X} \right\}. \end{aligned} \tag{7}$$

$\ell : \mathbb{N} \rightarrow \mathbb{N}$ and $\kappa : \mathbb{N} \rightarrow \mathbb{N}$ are two mapping functions that associate the indexes of the samples, contained inside \mathcal{X} , to their respective preferences in \mathcal{B} . The cardinalities of this sets are $|\mathcal{X}| = N$ and $|\mathcal{B}| = |\mathcal{S}| = M$. Also note that $1 \leq M \leq \binom{N}{2}$.

3 Handling exploration and exploitation

In this Section we review some key concepts that are common in most preference-based optimization algorithms. We also cover briefly how exploration and exploitation are handled by algorithm GLISp [3].

Preference-based surrogate-based methods iteratively propose new samples to try with the objective of solving Problem (3), while also minimizing the number of comparisons. Suppose that, *at iteration k*, we have at our disposal the set of samples \mathcal{X} , $|\mathcal{X}| = N$, and sets \mathcal{B} and \mathcal{S} . We define the best sample found so far by the procedure as

$$\begin{aligned} \mathbf{x}_{best}(N) &\in \mathbb{R}^n, \mathbf{x}_{best}(N) \in \mathcal{X}, |\mathcal{X}| = N, && \text{such that} \\ \mathbf{x}_{best}(N) &\succsim \mathbf{x}_i, \forall \mathbf{x}_i \in \mathcal{X}. \end{aligned}$$

The new candidate sample,

$$\mathbf{x}_{N+1} \in \mathbb{R}^n, \mathbf{x}_{N+1} \notin \mathcal{X},$$

is obtained by solving an additional optimization problem:

$$\begin{aligned} \mathbf{x}_{N+1} &= \arg \min_{\mathbf{x}} a(\mathbf{x}) \\ \text{s.t. } &\mathbf{x} \in \Omega, \end{aligned} \quad (8)$$

where $a : \mathbb{R}^n \rightarrow \mathbb{R}$ is a properly defined *acquisition function* which *trades off exploration and exploitation*.

In practice, once \mathbf{x}_{N+1} has been computed, we let the user express a preference between the best sample found so far and the new one, obtaining $b_{M+1} = \pi(\mathbf{x}_{N+1}, \mathbf{x}_{best}(N))$. After that, \mathbf{x}_{N+1} is added to the set \mathcal{X} and, similarly, sets \mathcal{B} and \mathcal{S} are also updated with the new preference b_{M+1} . The process is iterated until a certain condition is met. Usually, a *budget*, or rather a maximum number of samples to evaluate N_{max} , is set and the procedure is stopped once it is reached.

In our case, $a(\mathbf{x})$ in (8) is defined starting from a surrogate model $\hat{f} : \mathbb{R}^n \rightarrow \mathbb{R}$, which aims to approximate the scoring function $f(\mathbf{x})$, and a function $z : \mathbb{R}^n \rightarrow \mathbb{R}$ that promotes the exploration of the regions of Ω where few samples have been tried. The acquisition function that we will propose is an explicit trade-off between these two functions which, in its simplest form, can be written as:

$$a(\mathbf{x}) = \delta \cdot \hat{f}(\mathbf{x}) + (1 - \delta) \cdot z(\mathbf{x}), \quad (9)$$

where $\delta \in [0, 1]$ weighs the two terms. In practice, as we will show in Section 4, *the surrogate and the exploration functions need to be properly rescaled to make them comparable*. $\hat{f}(\mathbf{x})$ and $z(\mathbf{x})$ are defined as in GLISp [3], which we will now review briefly.

3.1 Surrogate model

Given N points $\mathbf{x}_i \in \mathcal{X}$, we define the surrogate model $\hat{f} : \mathbb{R}^n \rightarrow \mathbb{R}$ as the *radial basis function expansion* [9]:

$$\begin{aligned} \hat{f}(\mathbf{x}) &= \sum_{i=1}^N \beta^{(i)} \cdot \varphi(\epsilon \cdot \|\mathbf{x} - \mathbf{x}_i\|_2) \\ &= \sum_{i=1}^N \beta^{(i)} \cdot \phi_i(\mathbf{x}) \\ &= \boldsymbol{\phi}(\mathbf{x})^\top \cdot \boldsymbol{\beta}, \end{aligned} \quad (10)$$

where $\varphi : \mathbb{R}_{\geq 0} \rightarrow \mathbb{R}$ is a properly chosen *radial function*, $\epsilon \in \mathbb{R}_{>0}$ is the so-called *shape parameter* (which needs to be tuned) and $\phi_i : \mathbb{R}^n \rightarrow \mathbb{R}$ is the *radial basis function* originated from $\varphi(\cdot)$ and center $\mathbf{x}_i \in \mathcal{X}$, namely $\phi_i(\mathbf{x}) = \varphi(\epsilon \cdot \|\mathbf{x} - \mathbf{x}_i\|_2)$. Moreover, $\boldsymbol{\phi}(\mathbf{x}) \in \mathbb{R}^N$, $\boldsymbol{\phi}(\mathbf{x}) = [\phi_1(\mathbf{x}) \ \dots \ \phi_N(\mathbf{x})]^\top$, is the *radial basis function vector* and $\boldsymbol{\beta} = [\beta^{(1)} \ \dots \ \beta^{(N)}]^\top \in \mathbb{R}^N$ is a *vector of weights* that has to be computed based on the expressed preferences. Given a distance $r = \|\mathbf{x} - \mathbf{x}_i\|_2$, some commonly used radial functions are [10]:

- inverse quadratic: $\varphi(\epsilon \cdot r) = \frac{1}{1+(\epsilon \cdot r)^2}$;
- multiquadratic: $\varphi(\epsilon \cdot r) = \sqrt{1 + (\epsilon \cdot r)^2}$;
- linear: $\varphi(\epsilon \cdot r) = \epsilon \cdot r$;
- Gaussian: $\varphi(\epsilon \cdot r) = e^{-(\epsilon \cdot r)^2}$;
- thin plate spline: $\varphi(\epsilon \cdot r) = (\epsilon \cdot r)^2 \cdot \log(\epsilon \cdot r)$;
- inverse multiquadratic: $\varphi(\epsilon \cdot r) = \frac{1}{\sqrt{1+(\epsilon \cdot r)^2}}$.

One advantage of using model (10) as the surrogate model is highlighted by the following Theorem.

Theorem 2. *Function $\hat{f}(\mathbf{x})$ in (10) is differentiable everywhere³ with respect to \mathbf{x} if and only if the chosen radial basis function $\phi_i(\mathbf{x}) = \varphi(\epsilon \cdot \|\mathbf{x} - \mathbf{x}_i\|_2)$ is differentiable everywhere.*

If $\phi_i(\mathbf{x})$ in (10) is differentiable everywhere with respect to \mathbf{x} , then $\hat{f}(\mathbf{x})$ is a linear combination of differentiable functions, making it differentiable. Viceversa, if $\phi_i(\mathbf{x})$ is not differentiable everywhere, then the same can be said for the surrogate model in (10). For example, choosing $\phi_i(\mathbf{x}) = \|\epsilon \cdot (\mathbf{x} - \mathbf{x}_i)\|_2$ (linear radial function) results in a $\hat{f}(\mathbf{x})$ that is not differentiable for $\mathbf{x} = \mathbf{x}_i, \mathbf{x}_i \in \mathcal{X}$, since the Euclidean norm is not differentiable in $\mathbf{0}_n$.

It is also easy to prove the following Lemma.

Lemma 1. *The gradient of $\hat{f}(\mathbf{x})$ in (10) is*

$$\nabla_{\mathbf{x}} \hat{f}(\mathbf{x}) = \sum_{i=1}^N \beta^{(i)} \cdot \nabla_{\mathbf{x}} \phi_i(\mathbf{x}), \quad (11)$$

where $\nabla_{\mathbf{x}} \phi_i(\mathbf{x})$ is the gradient of the chosen radial basis function.

The surrogate model in (10) can be used to define the *surrogate preference function* $\hat{\pi} : \mathbb{R}^n \times \mathbb{R}^n \rightarrow \{-1, 0, 1\}$. Differently from $\pi(\mathbf{x}_i, \mathbf{x}_j)$ in (4), we consider a tolerance $\sigma \in \mathbb{R}_{>0}$ to avoid using strict inequalities and equalities and define $\hat{\pi}(\mathbf{x}_i, \mathbf{x}_j)$ as [3]:

$$\hat{\pi}(\mathbf{x}_i, \mathbf{x}_j) = \begin{cases} -1 & \text{if } \hat{f}(\mathbf{x}_i) - \hat{f}(\mathbf{x}_j) \leq -\sigma \\ 0 & \text{if } \left| \hat{f}(\mathbf{x}_i) - \hat{f}(\mathbf{x}_j) \right| \leq \sigma \\ 1 & \text{if } \hat{f}(\mathbf{x}_i) - \hat{f}(\mathbf{x}_j) \geq \sigma \end{cases} \quad (12)$$

Suppose now that, at iteration k of the optimization procedure, we have at our disposal sets \mathcal{X}, \mathcal{B} and \mathcal{S} . Then, we are interested in a surrogate model $\hat{f}(\mathbf{x})$ that correctly describes the expressed preferences, i.e. we would like the corresponding surrogate preference function $\hat{\pi}(\mathbf{x}_i, \mathbf{x}_j)$ to be such that

$$b_h = \hat{\pi}(\mathbf{x}_{\ell(h)}, \mathbf{x}_{\kappa(h)}), \forall b_h \in \mathcal{B}, (\ell(h), \kappa(h)) \in \mathcal{S}.$$

This, in turn, translates into some constraints on $\hat{f}(\mathbf{x})$ in (10), which can be used to find β . In order to do so, the authors of GLISp [3] define the following convex optimization problem:

$$\begin{aligned} & \arg \min_{\epsilon, \beta} \frac{\lambda}{2} \cdot \beta^\top \cdot \beta + \mathbf{g}^\top \cdot \epsilon & (13) \\ \text{s.t. } & \hat{f}(\mathbf{x}_{\ell(h)}) - \hat{f}(\mathbf{x}_{\kappa(h)}) \leq -\sigma + \epsilon^{(h)} & \forall h : b_h = -1 \\ & \left| \hat{f}(\mathbf{x}_{\ell(h)}) - \hat{f}(\mathbf{x}_{\kappa(h)}) \right| \leq \sigma + \epsilon^{(h)} & \forall h : b_h = 0 \\ & \hat{f}(\mathbf{x}_{\ell(h)}) - \hat{f}(\mathbf{x}_{\kappa(h)}) \geq \sigma - \epsilon^{(h)} & \forall h : b_h = 1 \\ & \epsilon \geq \mathbf{0}_M \\ & h = 1, \dots, M, \end{aligned}$$

where:

- $\epsilon = [\epsilon^{(1)} \dots \epsilon^{(M)}]^\top \in \mathbb{R}^M$ is a vector of *slack variables* (one for each preference) which takes into consideration that (i) there might be some outliers in \mathcal{B} and \mathcal{S} if the human decision-maker expresses the preferences in an inconsistent way and (ii) the selected radial function and/or shape parameter do not allow a proper approximation of the scoring function $f(\mathbf{x})$;
- $\mathbf{g} = [g^{(1)} \dots g^{(M)}]^\top \in \mathbb{R}_{>0}^M$ is a vector of weights which can be used to penalize more some slacks related to the most important preferences;
- $\lambda \in \mathbb{R}_{\geq 0}$ plays the role of a *regularization parameter*. It is easy to see that, for $\lambda = 0$, Problem (13) is a Linear Program (LP) while, for $\lambda > 0$, it is a Quadratic Program (QP).

³Note that, whenever we say that a multivariate function, such as $\hat{f}(\mathbf{x})$, is “differentiable everywhere”, we imply that it is differentiable $\forall \mathbf{x} \in \mathbb{R}^n$.

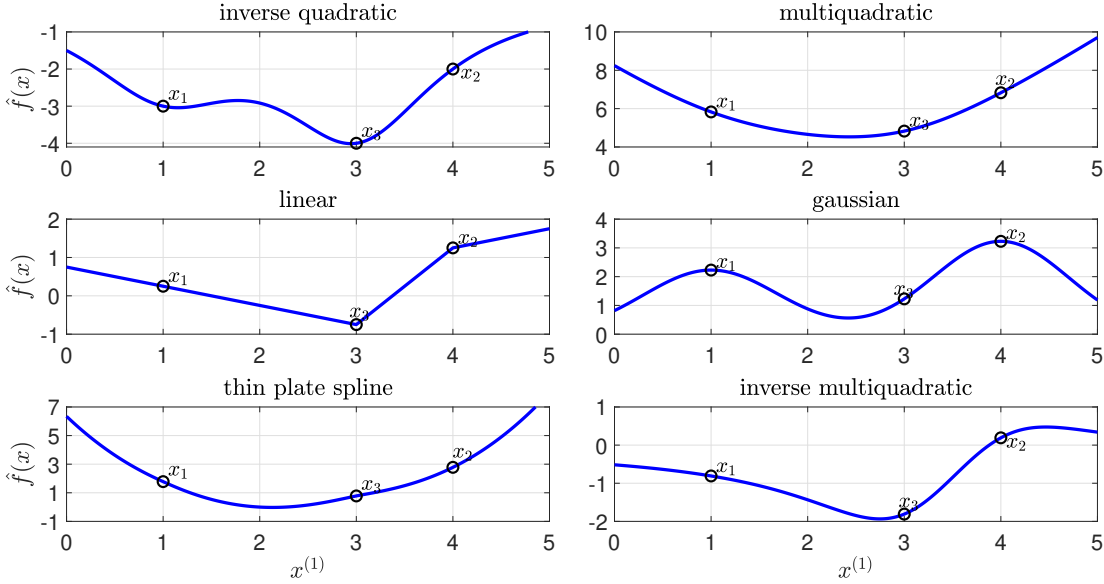


Figure 1: Examples of surrogate functions $\hat{f}(x)$ in (10) originated from different radial functions $\varphi(\cdot)$ with $\epsilon = 1$ and hyperparameters of Problem (13): $\sigma = 1, \lambda = 0$ and $\mathbf{g} = [1, 1, 1]^\top$. All weight vectors β for $\hat{f}(x)$ have been computed using three samples, $\mathcal{X} = \{x_1 = 1, x_2 = 4, x_3 = 3\}$, preferences $\mathcal{B} = \{b_1 = -1, b_2 = 1, b_3 = 1\}$ and mapping set $\mathcal{S} = \{(1, 2), (2, 3), (1, 3)\}$. In practice, these sets define the following ordering for the samples: $x_3 \succ x_1 \succ x_2$, which equates to a scoring function such that $f(x_3) < f(x_1) < f(x_2)$. Notice how all surrogates maintain the same ordering for the samples, i.e. they capture the given preferences.

Problem (13) ensures that, at least approximately, $\hat{f}(x)$ is a suitable representation of the unknown preference relation \succsim which generated the data (see Theorem 1). Some examples of surrogate functions for different choices of the radial function $\varphi(\cdot)$ are depicted in Figure 1.

Recall that the goal of preference-based optimization is not to approximate the scoring function in the best way possible, but to converge to \mathbf{x}^* with the least amount of comparisons. Therefore, the preferences related to $\mathbf{x}_{best}(N)$ at the current iteration are more important than the others, making us interested in satisfying them without any slack. In order to do so, we define vector \mathbf{g} as it has been done in the original implementation of GLISp [3]:

$$\begin{aligned} g^{(h)} &= 1, \quad \forall h : (\ell(h), \kappa(h)) \in \mathcal{S}, \mathbf{x}_{\ell(h)} \neq \mathbf{x}_{best}(N) \text{ and } \mathbf{x}_{\kappa(h)} \neq \mathbf{x}_{best}(N), \\ g^{(h)} &= 10, \quad \forall h : (\ell(h), \kappa(h)) \in \mathcal{S}, \mathbf{x}_{\ell(h)} = \mathbf{x}_{best}(N) \text{ or } \mathbf{x}_{\kappa(h)} = \mathbf{x}_{best}(N), \end{aligned}$$

penalizing more the slacks associated to the preferences expressed for the current best sample.

3.2 Exploration function

Given a sample $\mathbf{x}_i \in \mathcal{X}$, consider the *inverse distance weighting function* (IDW) $w_i : \mathbb{R}^n \setminus \{\mathbf{x}_i\} \rightarrow \mathbb{R}_{>0}$ defined as in [28]:

$$w_i(\mathbf{x}) = \frac{1}{\|\mathbf{x} - \mathbf{x}_i\|_2^2}. \quad (14)$$

GLISp [3] uses the so-called *IDW distance function* $z : \mathbb{R}^n \rightarrow (-1, 0]$, defined as:

$$z(\mathbf{x}) = \begin{cases} 0 & \text{if } \mathbf{x} \in \mathcal{X} \\ -\frac{2}{\pi} \cdot \arctan\left(\frac{1}{\sum_{i=1}^N w_i(\mathbf{x})}\right) & \text{otherwise} \end{cases}, \quad (15)$$

to promote the exploration of the regions of \mathbb{R}^n where few samples are present based only on the points in \mathcal{X} . Moreover, it is possible to prove the following Theorem and Lemma.

Theorem 3 ([2]). *The IDW distance function $z(\mathbf{x})$ in (15) is differentiable everywhere.*

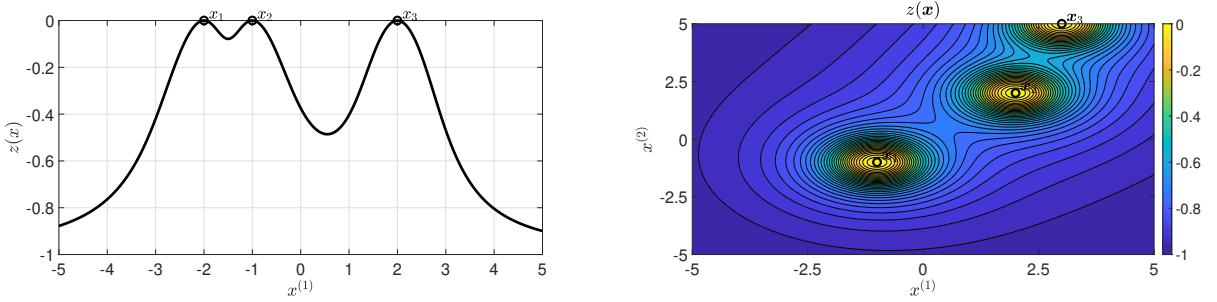


Figure 2: Examples of the IDW distance function in (15) for $N = 3$ points in case of a one-dimensional (left) and two-dimensional (right) decision variable. Notice how $z(\mathbf{x})$ assumes its lowest values the furthest away from the locations of the samples in \mathcal{X} .

Lemma 2. *The gradient of the IDW distance function $z(\mathbf{x})$ in (15) is:*

$$\nabla_{\mathbf{x}} z(\mathbf{x}) = \begin{cases} \mathbf{0}_n & \text{if } \mathbf{x} \in \mathcal{X} \\ -\frac{4}{\pi} \cdot \frac{\sum_{i=1}^N (\mathbf{x} - \mathbf{x}_i) \cdot w_i(\mathbf{x})^2}{1 + [\sum_{i=1}^N w_i(\mathbf{x})]^2} & \text{otherwise} \end{cases} \quad (16)$$

The proof of Theorem 3 is given in [2]. Here, we provide the proof for Lemma 2 in Appendix A. The gradient $\nabla_{\mathbf{x}} z(\mathbf{x})$ in (16) will be particularly relevant in the following Section.

Some examples of the IDW distance function are depicted in Figure 2.

4 Next candidate sample search

As previously mentioned in Section 3, a key aspect of surrogate-based methods is the exploration-exploitation trade-off. In practice, simply defining an acquisition function as in (9) does not constitute the best course of action because $\hat{f}(\mathbf{x})$ and $z(\mathbf{x})$ often exhibit different ranges, making them not comparable. Instead, in [3], the authors propose the following $a(\mathbf{x})$ for GLISp:

$$a(\mathbf{x}) = \frac{\hat{f}(\mathbf{x})}{\Delta \hat{F}(\mathcal{X})} + \delta \cdot z(\mathbf{x}), \quad (17)$$

where $\delta \in \mathbb{R}_{\geq 0}$ defines the exploration-exploitation trade-off. The division by $\Delta \hat{F}(\mathcal{X}) = \max_{\mathbf{x} \in \mathcal{X}} \hat{f}(\mathbf{x}) - \min_{\mathbf{x} \in \mathcal{X}} \hat{f}(\mathbf{x})$ aims to rescale the surrogate function as to make it comparable to the range of the IDW distance function in (15) (which is $(-1, 0]$).

In this Section we are going to address some limitations of $z(\mathbf{x})$, which might prevent procedure GLISp [3] from reaching the global minimizer of Problem (3), and define an alternative acquisition function compared to the one in (17). Furthermore, we propose a strategy to iteratively modify the exploration-exploitation trade-off.

4.1 Improving the exploration capabilities of $z(\mathbf{x})$

The main shortcomings of $z(\mathbf{x})$ in (15) are:

1. Even though the codomain of $z(\mathbf{x})$ is $(-1, 0]$, what we are really interested in (to solve Problem (3) and Problem (8)) are the values that it assumes for $\mathbf{x} \in \Omega$ and not on its whole domain \mathbb{R}^n . In particular, there are some situations for which $|z(\mathbf{x})| \ll 1, \forall \mathbf{x} \in \Omega$, making its contribution in the acquisition function (9) negligible. Consider, for example, the case $\mathcal{X} = \{\mathbf{x}_1\}$, then, $\forall \mathbf{x} \notin \mathcal{X}$, the IDW distance function simply becomes

$$z(\mathbf{x}) = -\frac{2}{\pi} \cdot \arctan \left(\|\mathbf{x} - \mathbf{x}_1\|_2 \right).$$

Suppose that Problem (3) is only bound constrained, i.e. $\Omega = \{\mathbf{x} : \mathbf{l} \leq \mathbf{x} \leq \mathbf{u}\}$, then $z(\mathbf{x})$ assumes its lowest value at either $\mathbf{x} = \mathbf{l}$ or $\mathbf{x} = \mathbf{u}$. Clearly, if $\|\mathbf{l} - \mathbf{x}_1\|_2$ and $\|\mathbf{u} - \mathbf{x}_1\|_2$ are close to zero, then $|z(\mathbf{x})| \ll 1, \forall \mathbf{x} \in \Omega$. Similarly, even if the acquisition function is defined as in (17), unless $\delta \gg 1$, $\hat{f}(\mathbf{x})$ and $z(\mathbf{x})$ might not be comparable.

2. The values assumed by the IDW distance function tend to “shrink” as the number of samples increases. To clarify this, consider two sets of samples:

$$\begin{aligned}\mathcal{X}' &= \{\mathbf{x}_1, \dots, \mathbf{x}_N\}, \\ \mathcal{X}'' &= \mathcal{X}' \cup \{\mathbf{x}_{N+1}\}.\end{aligned}$$

Given any point $\tilde{\mathbf{x}} \notin \mathcal{X}''$, the IDW distance functions obtained from the previously defined sets are:

$$\begin{aligned}z_{\mathcal{X}'}(\tilde{\mathbf{x}}) &= -\frac{2}{\pi} \cdot \arctan\left(\frac{1}{\sum_{i=1}^N w_i(\tilde{\mathbf{x}})}\right), \\ z_{\mathcal{X}''}(\tilde{\mathbf{x}}) &= -\frac{2}{\pi} \cdot \arctan\left(\frac{1}{\sum_{i=1}^{N+1} w_i(\tilde{\mathbf{x}})}\right),\end{aligned}$$

where the subscripts of $z(\mathbf{x})$ in the previous equations indicate the sample set that is used to define them. Then, since $w_i(\tilde{\mathbf{x}}) > 0, \forall \tilde{\mathbf{x}} \notin \mathcal{X}''$ and $i = 1, \dots, N + 1$, we have

$$|z_{\mathcal{X}'}(\tilde{\mathbf{x}})| > |z_{\mathcal{X}''}(\tilde{\mathbf{x}})| > 0,$$

proving the above point. In practice, this means that the optimization algorithm will explore less as the number of sample increases.

A visualization of these two aspects is presented in Figure 3.

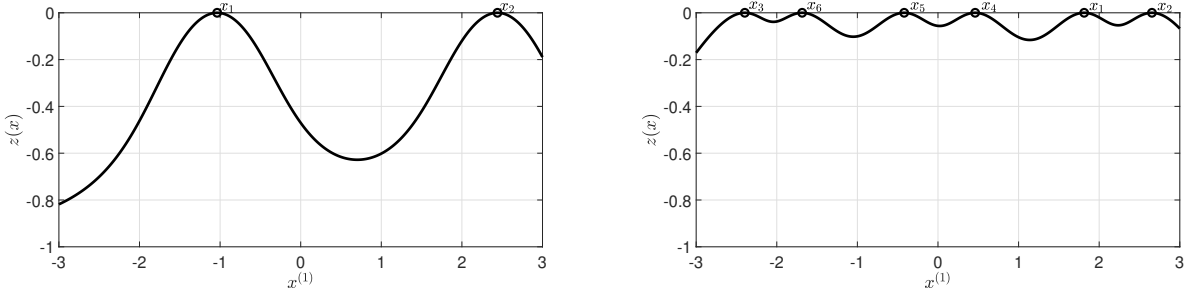


Figure 3: Examples of the IDW distance function $z(x)$ in (15) for a different number of points ($N = 2$ on the left, $N = 6$ on the right) and $-3 = l \leq x \leq u = 3$. Notice how $z(x)$ does not cover the whole range $(-1, 0]$, at least inside the domain imposed by the bound constraints, and its values “shrink” as the number of samples increases.

Clearly, the previous two observations highlight how an acquisition function defined as in (9) could potentially fail, since the exploration and exploitation terms are not directly comparable. Moreover, unlike $z(\mathbf{x})$, the range of $\hat{f}(\mathbf{x})$ is not a-priori known. Therefore, the exploration and exploitation functions need to be properly rescaled in order to obtain a better suited acquisition function. As previously pointed out, in GLISp [3] the authors rescale $\hat{f}(\mathbf{x})$ as in (17). Instead, here, we aim to define an acquisition function that is similar to the one used for the Metric Stochastic Response Surface (MSRS) [26] algorithm, a popular black-box optimization procedure. In MSRS [26], the surrogate $\hat{f}(\mathbf{x})$ and the exploration function $z(\mathbf{x})$ (which is defined differently from the one in (15)) are made comparable by randomly sampling Ω and rescaling the two using min-max normalization. Then, Problem (8) is not solved explicitly but by choosing the generated random sample that achieves the lowest value for the acquisition function.

In this work, we propose to *rescale* $z(\mathbf{x})$ and $\hat{f}(\mathbf{x})$ using *some insights on the stationary points of the IDW distance function* and solve Problem (8) explicitly, using a proper optimization solver.

4.1.1 Stationary points for the IDW distance function

The locations of the global maximizers of $z(\mathbf{x})$ can be deduced immediately from (15) and Lemma 2 as stated by the following Proposition (see Appendix A for a formal proof).

Proposition 2. $\forall \mathbf{x}_i \in \mathcal{X}$ are global maximizers of $z(\mathbf{x})$.

Reaching similar conclusions for the minimizers of $z(\mathbf{x})$ is much harder, however we can consider some simplified situations. Note that we are not necessarily interested in finding the minimizers of $z(\mathbf{x})$ with high accuracy, but rather to gain some insights on where they are likely to be located so that we can rescale both $z(\mathbf{x})$ and $\hat{f}(\mathbf{x})$ sufficiently enough to make them comparable. Moreover, their approximate locations can be used to solve the following optimization problem (*pure exploration*):

$$\begin{aligned} \mathbf{x}_{N+1} &= \arg \min_{\mathbf{x}} z(\mathbf{x}) \\ \text{s.t. } \mathbf{x} &\in \Omega \end{aligned} \quad (18)$$

by using a *multi-start derivative-based* (recall that $z(\mathbf{x})$ is differentiable everywhere, as proven by Theorem 3) *optimization procedure with warm-start* [23, 21]. Problem (18) is quite relevant for the convergence of the algorithm that we will propose in Section 5.

Remark 1. *In the following paragraphs we are going to analyze where the local minimizers of $z(\mathbf{x})$ in (15), as well as the solution(s) of the simplified problem*

$$\begin{aligned} \mathbf{x}_{N+1} &= \arg \min_{\mathbf{x}} z(\mathbf{x}) \\ \text{s.t. } \mathbf{l} &\leq \mathbf{x} \leq \mathbf{u} \end{aligned} \quad (19)$$

are located in some specific cases. In practice, since $\{\mathbf{x} : \mathbf{l} \leq \mathbf{x} \leq \mathbf{u}\} \subseteq \Omega$, the global minima $z(\mathbf{x}_{N+1})$ of Problem (19) is lower or at most equal to the global minima of Problem (18). Therefore, the minimizers of Problem (19) are better suited to perform min-max rescaling of $z(\mathbf{x})$ than the ones of Problem (18).

Case $\mathcal{X} = \{\mathbf{x}_1\}$ ($N = 1$)

The IDW distance function and its gradient $\forall \mathbf{x} \notin \mathcal{X}$ are:

$$\begin{aligned} z(\mathbf{x}) &= -\frac{2}{\pi} \cdot \arctan\left(\|\mathbf{x} - \mathbf{x}_1\|_2\right), \\ \nabla_{\mathbf{x}} z(\mathbf{x}) &= -\frac{4}{\pi} \cdot (\mathbf{x} - \mathbf{x}_1) \cdot \frac{w_1(\mathbf{x})^2}{1 + w_1(\mathbf{x})^2}. \end{aligned}$$

Clearly, $\forall \mathbf{x} \notin \mathcal{X}$, the gradient is never zero since $w_1(\mathbf{x}) > 0$. Therefore, the only stationary point is the global maximizer \mathbf{x}_1 . However, if we were to consider Problem (19), then its solution would be located either at \mathbf{l} or \mathbf{u} .

Case $\mathcal{X} = \{\mathbf{x}_1, \mathbf{x}_2\}$ ($N = 2$)

The gradient of the IDW distance function $\forall \mathbf{x} \notin \mathcal{X}$ is:

$$\nabla_{\mathbf{x}} z(\mathbf{x}) = -\frac{4}{\pi} \cdot \frac{(\mathbf{x} - \mathbf{x}_1) \cdot w_1(\mathbf{x})^2 + (\mathbf{x} - \mathbf{x}_2) \cdot w_2(\mathbf{x})^2}{1 + [w_1(\mathbf{x}) + w_2(\mathbf{x})]^2}.$$

Let us consider the midpoint $\mathbf{x}_{\mu} = \frac{\mathbf{x}_1 + \mathbf{x}_2}{2}$, that is such that $\|\mathbf{x}_{\mu} - \mathbf{x}_1\|_2 = \|\mathbf{x}_{\mu} - \mathbf{x}_2\|_2$ and for which $w_1(\mathbf{x}_{\mu}) = w_2(\mathbf{x}_{\mu})$. If we substitute it in the previous expression, we obtain:

$$\nabla_{\mathbf{x}} z(\mathbf{x}_{\mu}) = \mathbf{0}_n,$$

which means that \mathbf{x}_{μ} is a stationary point for $z(\mathbf{x})$. It is easy to see by visual inspection that such point is actually a local minimizer for the IDW distance function (see, for example, Figure 4). Note that \mathbf{x}_{μ} is not necessarily the global solution of Problem (19), it might just be a local one.

Case $\mathcal{X} = \mathcal{X}^{(1)} \cup \mathcal{X}^{(2)}$ ($N > 2$)

Suppose now that the samples contained in \mathcal{X} can be divided into two clusters:

- $\mathcal{X}^{(1)} = \{\mathbf{x}_1, \dots, \mathbf{x}_{N_1}\}$ ($|\mathcal{X}^{(1)}| = N_1$),
- $\mathcal{X}^{(2)} = \{\mathbf{x}_{N_1+1}, \dots, \mathbf{x}_N\}$ ($|\mathcal{X}^{(2)}| = N - N_1$),

such that $\mathcal{X}^{(1)} \cap \mathcal{X}^{(2)} = \emptyset$ and $\mathcal{X}^{(1)} \cup \mathcal{X}^{(2)} = \mathcal{X}$. Consider the midpoint between the centroids of each cluster:

$$\mathbf{x}_{\mu} = \frac{1}{2} \cdot \left[\frac{\sum_{\mathbf{x}_i \in \mathcal{X}^{(1)}} \mathbf{x}_i}{N_1} + \frac{\sum_{\mathbf{x}_i \in \mathcal{X}^{(2)}} \mathbf{x}_i}{N - N_1} \right]. \quad (20)$$

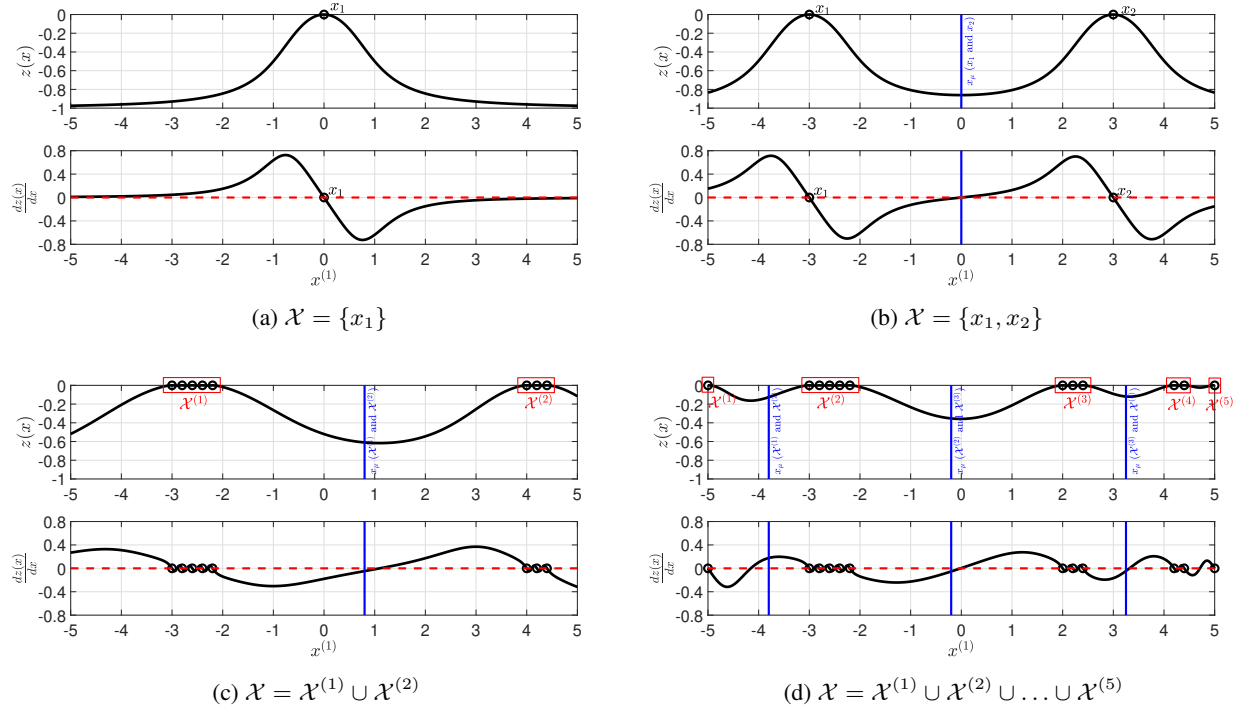


Figure 4: Examples of the IDW distance function (15) and its gradient (16) in the four analyzed cases. The red boxes mark the different clusters while the red dashed line highlights the values of \mathbf{x} for which the first derivative is zero. Finally, the blue vertical lines mark the midpoints (either between points or clusters). Only a portion of all possible midpoints between centroids has been reported in the general case. Even though all the previously seen simplifying assumptions do not hold completely for 4c and 4d, the midpoints turn out to be quite close to the local minimizers of $z(\mathbf{x})$.

We make the simplifying assumption that all points contained inside each cluster are quite close to each other, i.e. $\mathbf{x}_1 \approx \mathbf{x}_2 \approx \dots \approx \mathbf{x}_{N_1}$ and $\mathbf{x}_{N_1+1} \approx \mathbf{x}_{N_1+2} \approx \dots \approx \mathbf{x}_N$. Then, the midpoint in (20) is approximately equal to $\mathbf{x}_\mu \approx \frac{\mathbf{x}_1 + \mathbf{x}_N}{2}$. Now, let us evaluate the gradient of the IDW distance function at \mathbf{x}_μ :

$$\nabla_{\mathbf{x}} z(\mathbf{x}_\mu) = -\frac{4}{\pi} \cdot \frac{\sum_{i=1}^N (\mathbf{x}_\mu - \mathbf{x}_i) \cdot w_i(\mathbf{x}_\mu)^2}{1 + \left[\sum_{i=1}^N w_i(\mathbf{x}_\mu) \right]^2}.$$

Using the previous assumption, we have that $w_1(\mathbf{x}_\mu) \approx \dots \approx w_{N_1}(\mathbf{x}_\mu) \approx w_{N_1+1}(\mathbf{x}_\mu) \approx \dots \approx w_N(\mathbf{x}_\mu)$ and thus the gradient becomes:

$$\nabla_{\mathbf{x}} z(\mathbf{x}_\mu) \approx -\frac{4}{\pi} \cdot \frac{w_1(\mathbf{x}_\mu)^2}{1 + [N \cdot w_1(\mathbf{x}_\mu)]^2} \cdot \left[\left(\frac{N}{2} - N_1 \right) \cdot \mathbf{x}_1 + \left(-\frac{N}{2} + N_1 \right) \cdot \mathbf{x}_N \right].$$

Clearly, if the clusters are nearly equally sized, i.e. $N_1 \approx N - N_1 \approx \frac{N}{2}$, then

$$\nabla_{\mathbf{x}} z(\mathbf{x}_\mu) \approx \mathbf{0}_n,$$

reaching a similar result to the one that we have seen for the case $N = 2$. The quality of this approximation depends on whether the simplifying assumptions are satisfied or not (and to what degree).

General case ($N > 2$)

Any set of samples \mathcal{X} can be partitioned into an arbitrary number of disjoint clusters, say $K \in \mathbb{N}$, i.e.

$$\mathcal{X} = \mathcal{X}^{(1)} \cup \mathcal{X}^{(2)} \cup \dots \cup \mathcal{X}^{(K)}, \mathcal{X}^{(i)} \cap \mathcal{X}^{(j)} = \emptyset, \forall i \neq j,$$

where K is at most N . In this case, finding local solutions explicitly, or even approximately, is quite complex. Heuristically speaking, if the clusters are “well spread” (i.e. all the points contained inside each cluster $\mathcal{X}^{(i)}$ are

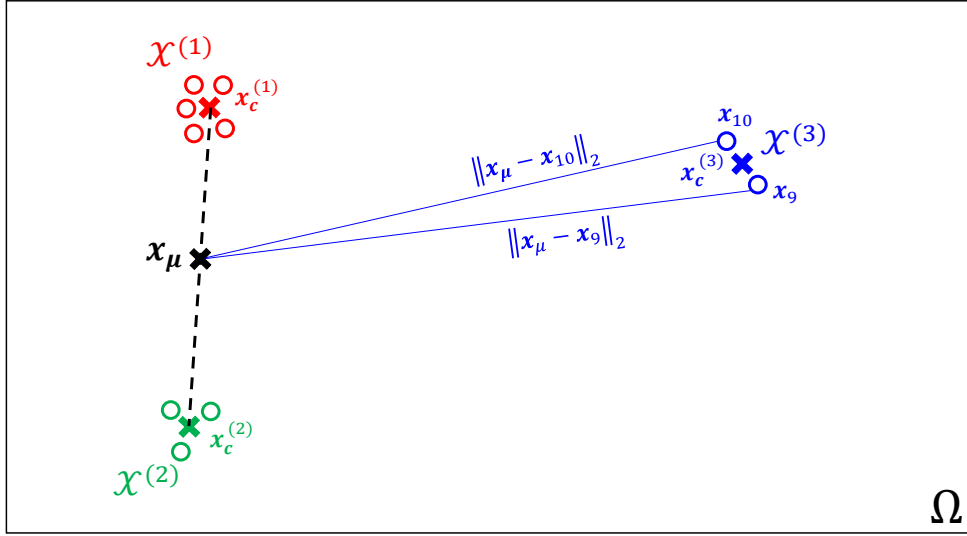


Figure 5: Two-dimensional example of “well spread” clusters, highlighted with different colors. The circles denote the points contained in \mathcal{X} while the crosses represent the centroids of $\mathcal{X}^{(1)}$, $\mathcal{X}^{(2)}$ and $\mathcal{X}^{(3)}$. \mathbf{x}_μ is the midpoint between the centroids of clusters $\mathcal{X}^{(1)}$ and $\mathcal{X}^{(2)}$. Finally, the blue lines highlight the distances between the samples of cluster $\mathcal{X}^{(3)}$ and \mathbf{x}_μ .

sufficiently far away from the other ones in $\mathcal{X}^{(j)}$, $j = 1, \dots, K, j \neq i$), then we can approximately deduce where the local minimizers of $z(\mathbf{x})$ are. For instance, Figure 5 depicts a set of samples \mathcal{X} that has been partitioned into three clusters, $\mathcal{X}^{(1)}$, $\mathcal{X}^{(2)}$ and $\mathcal{X}^{(3)}$, and for which the former hypothesis is satisfied. Let us write $z(\mathbf{x})$ by considering the contribution of each cluster explicitly and in the case $\mathbf{x} \notin \mathcal{X}$:

$$z(\mathbf{x}) = -\frac{2}{\pi} \cdot \arctan \left[\left(\sum_{\mathbf{x}_i \in \mathcal{X}^{(1)}} \frac{1}{\|\mathbf{x} - \mathbf{x}_i\|_2^2} + \sum_{\mathbf{x}_i \in \mathcal{X}^{(2)}} \frac{1}{\|\mathbf{x} - \mathbf{x}_i\|_2^2} + \sum_{\mathbf{x}_i \in \mathcal{X}^{(3)}} \frac{1}{\|\mathbf{x} - \mathbf{x}_i\|_2^2} \right)^{-1} \right].$$

In the general case, given $\mathcal{X}^{(i)}$ and $\mathcal{X}^{(j)}$, we define their centroids $\mathbf{x}_c^{(i)}$, $\mathbf{x}_c^{(j)}$, and the corresponding midpoint \mathbf{x}_μ between them as:

$$\mathbf{x}_c^{(k)} = \frac{\sum_{\mathbf{x}_i \in \mathcal{X}^{(k)}} \mathbf{x}_i}{|\mathcal{X}^{(k)}|} \quad \text{centroid of } k\text{-th cluster,} \quad (21)$$

$$\mathbf{x}_\mu = \frac{\mathbf{x}_c^{(i)} + \mathbf{x}_c^{(j)}}{2} \quad \text{midpoint.} \quad (22)$$

Going back to the example depicted in Figure 5, if we consider the midpoint \mathbf{x}_μ between the centroids of $\mathcal{X}^{(1)}$ and $\mathcal{X}^{(2)}$, using the “well spread” hypothesis we can say that $\|\mathbf{x}_\mu - \mathbf{x}_i\|_2 \gg 0, \forall \mathbf{x}_i \in \mathcal{X}^{(3)}$, making the contributions of the points inside the third cluster negligible when evaluating $z(\mathbf{x})$ at \mathbf{x}_μ . Formally:

$$z(\mathbf{x}_\mu) \approx -\frac{2}{\pi} \cdot \arctan \left[\left(\sum_{\mathbf{x}_i \in \mathcal{X}^{(1)}} \frac{1}{\|\mathbf{x}_\mu - \mathbf{x}_i\|_2^2} + \sum_{\mathbf{x}_i \in \mathcal{X}^{(2)}} \frac{1}{\|\mathbf{x}_\mu - \mathbf{x}_i\|_2^2} \right)^{-1} \right].$$

Some similar considerations can be made for the gradient $\nabla_{\mathbf{x}} z(\mathbf{x})$ at \mathbf{x}_μ . In general, given K clusters, if these are “well spread”, then we can consider each possible couple of clusters separately and neglect the contributions of the remaining ones. Therefore, approximately speaking, we reach the same conclusion to the one that we have seen in the previous case, namely that the local minima are likely located near the midpoints between the centroids of each couple of clusters.

Some scalar examples of all these situations are reported in Figure 4.

4.1.2 Min-max rescaling and augmented sample set

Given a set of samples \mathcal{X} and a generic multivariate function $h : \mathbb{R}^n \rightarrow \mathbb{R}$, *min-max rescaling* (or normalization) [16] rescales $h(\mathbf{x})$ as:

$$\bar{h}(\mathbf{x}) = \frac{h(\mathbf{x}) - h_{\min}(\mathcal{X})}{\Delta H(\mathcal{X})}, \quad (23)$$

where

$$h_{\min}(\mathcal{X}) = \min_{\mathbf{x} \in \mathcal{X}} h(\mathbf{x}), \quad (24a)$$

$$h_{\max}(\mathcal{X}) = \max_{\mathbf{x} \in \mathcal{X}} h(\mathbf{x}), \quad (24b)$$

$$\Delta H(\mathcal{X}) = h_{\max}(\mathcal{X}) - h_{\min}(\mathcal{X}). \quad (24c)$$

Note that, to avoid dividing by zero in (23), $\Delta H(\mathcal{X})$ can be set to $h_{\max}(\mathcal{X})$ or 1 whenever $h_{\min}(\mathcal{X}) = h_{\max}(\mathcal{X}) \neq 0$ or $h_{\min}(\mathcal{X}) = h_{\max}(\mathcal{X}) = 0$ respectively.

The objective of min-max rescaling is to obtain a function with range $[0, 1]$, i.e. we would like to have $\bar{h} : \mathbb{R}^n \rightarrow [0, 1]$. Clearly, the quality of the normalization depends on the information brought by the samples contained inside \mathcal{X} , as pointed out in the following Proposition.

Proposition 3. *We can observe that:*

1. *If \mathcal{X} contains both the global minimizer and maximizer of $h(\mathbf{x})$, then $\bar{h}(\mathbf{x})$ defined as in (23) effectively has codomain $[0, 1]$,*
2. *Otherwise, we can only ensure that $0 \leq \bar{h}(\mathbf{x}_i) \leq 1, \forall \mathbf{x}_i \in \mathcal{X}$.*
3. *In general, if we increase the amount of distinct samples in \mathcal{X} , then the rescaling of $h(\mathbf{x})$ gets better (or, worst case, stays the same).*

Going back to the problem of rescaling the IDW distance function $z(\mathbf{x})$ in (15), if we were to apply (23) using the set of previously evaluated samples \mathcal{X} , then it would not be effective since $z(\mathbf{x}_i) = 0, \forall \mathbf{x}_i \in \mathcal{X}$ (see Proposition 2). Instead, we have opted to generate a sufficiently expressive *augmented sample set* $\mathcal{X}_{aug} \supset \mathcal{X}$ and perform min-max normalization using \mathcal{X}_{aug} instead of \mathcal{X} .

Consider the general case described in Section 4.1.1, then the augmented sample set \mathcal{X}_{aug} can be built in the following fashion:

1. Partition the points in \mathcal{X} into different clusters. Here, for simplicity, we have fixed a-priori the number $K_{aug} > 1$ of clusters and we have applied K -means clustering [11, 5] to obtain the sets $\mathcal{X}^{(1)}, \dots, \mathcal{X}^{(K_{aug})}$.
2. Compute the centroids of each cluster, using (21), and group them inside the set $\mathcal{X}_c = \{\mathbf{x}_c^{(1)}, \dots, \mathbf{x}_c^{(K_{aug})}\}$.
3. Calculate all the midpoints \mathbf{x}_μ between each possible couple of centroids $\mathbf{x}_c^{(i)}, \mathbf{x}_c^{(j)} \in \mathcal{X}_c$ using (22). As we have seen in Section 4.1.1, if the “well spread” hypothesis holds, the midpoints are likely to be close to the minimizers of $z(\mathbf{x})$.
4. Build the augmented sample set as $\mathcal{X}_{aug} = \mathcal{X} \cup \mathcal{X}_\mu$, where \mathcal{X}_μ is the set which groups all the previously computed midpoints. Clearly, as highlighted by (23) and Proposition 3, if \mathcal{X}_{aug} contains points that are close (or equal) to the global minimizers and maximizers of $z(\mathbf{x})$, then the quality of the rescaling of the IDW distance function improves.

Algorithm 1 formalizes these steps while also taking into consideration the case $|\mathcal{X}| \leq K_{aug}$ (for which no clustering is performed). Note that we also include the bounds \mathbf{l} and \mathbf{u} inside \mathcal{X}_c and \mathcal{X}_{aug} for two reasons: (i) \mathbf{l} or \mathbf{u} might actually be the solution of Problem (19) (as we have seen in Section 4.1.1) and (ii) given that we also want to rescale $\hat{f}(\mathbf{x})$, adding additional points in the augmented sample set improves the quality of min-max normalization (see Proposition 3). The number of points contained inside \mathcal{X}_{aug} obtained from Algorithm 1 is:

$$|\mathcal{X}_{aug}| = |\mathcal{X}| + \binom{K_{aug} + 2}{2} + 2.$$

Therefore, to avoid excessively large augmented sample sets, K_{aug} needs to be chosen appropriately.

As a final remark, we point out that we could perform min-max normalization in (23) by using the real minima and maxima of $z(\mathbf{x})$ and $\hat{f}(\mathbf{x})$, which can be obtained by solving four additional global optimization problems.

However, we have preferred to stick with the proposed heuristic way since we are not interested in an extremely accurate rescaling and, also, to avoid potentially large overhead times due to solving extra optimization problems.

Algorithm 1 Computation of \mathcal{X}_{aug} for min-max scaling

Input:

- (i) Set of samples \mathcal{X} in (5),
- (ii) Number of clusters K_{aug} ,
- (iii) Bound constraints of the optimization problem \mathbf{u}, \mathbf{l} (see (1)).

Output:

- (i) Augmented sample set \mathcal{X}_{aug} to use for rescaling.

```

1: if  $|\mathcal{X}| > K_{aug}$  then
2:   Perform  $K$ -means clustering [11, 5] to group the data into  $K_{aug}$  clusters  $\mathcal{X}^{(1)}, \dots, \mathcal{X}^{(K_{aug})}$ 
3:   Compute the set of centroids  $\mathcal{X}_c$  using (21):
   
$$\mathcal{X}_c = \left\{ \mathbf{x}_k : \mathbf{x}_k = \mathbf{x}_c^{(k)} = \frac{\sum_{\mathbf{x}_i \in \mathcal{X}^{(k)}} \mathbf{x}_i}{|\mathcal{X}^{(k)}|}, k = 1, \dots, K_{aug} \right\}$$

4: else
5:   Set  $\mathcal{X}_c = \mathcal{X}$ 
6: Add the bound constraints to  $\mathcal{X}_c$ :  $\mathcal{X}_c = \mathcal{X}_c \cup \{\mathbf{l}, \mathbf{u}\}$ 
7: Group all possible couples of  $\mathcal{X}_c$  (without repetition):
   
$$\mathcal{X}_{couples} = \{(\mathbf{x}_i, \mathbf{x}_j) : \mathbf{x}_i, \mathbf{x}_j \in \mathcal{X}_c, \mathbf{x}_i \neq \mathbf{x}_j\}$$

8: Calculate the midpoints of all the couples inside  $\mathcal{X}_{couples}$ , obtaining the set:
   
$$\mathcal{X}_\mu = \left\{ \mathbf{x}_\mu : \mathbf{x}_\mu = \frac{\mathbf{x}_i + \mathbf{x}_j}{2}, (\mathbf{x}_i, \mathbf{x}_j) \in \mathcal{X}_{couples} \right\}$$

9: Build the augmented sample set as  $\mathcal{X}_{aug} = \mathcal{X} \cup \mathcal{X}_\mu \cup \{\mathbf{l}, \mathbf{u}\}$ 

```

4.2 Definition of the acquisition function

Instead of using acquisition function in (9) or the one employed for GLISp [3] in (17), we take advantage of the results on the stationary points of $z(\mathbf{x})$ presented in Section 4.1 to rescale the surrogate and the exploration function. In particular, we define the following acquisition function:

$$a(\mathbf{x}) = \delta \cdot \frac{\hat{f}(\mathbf{x}) - \hat{f}_{min}(\mathcal{X}_{aug})}{\Delta \hat{F}(\mathcal{X}_{aug})} + (1 - \delta) \cdot \frac{z(\mathbf{x}) - z_{min}(\mathcal{X}_{aug})}{\Delta Z(\mathcal{X}_{aug})}, \quad (25)$$

where \mathcal{X}_{aug} is the augmented sample set obtained by Algorithm 1 and $\delta \in [0, 1]$ is an hyperparameter that regulates the trade-off between exploration and exploitation. In particular, $\delta = 0$ corresponds to pure exploration, while $\delta = 1$ results in pure exploitation. $a(\mathbf{x})$ in (25) is similar to the acquisition function of MSRS [26] but here we use an ad-hoc augmented sample set instead of a randomly generated one and a different exploration function. We will refer to the algorithm that we will propose in Section 5, which uses $a(\mathbf{x})$ in (25), as GLISp-r, where “r” highlights the min-max rescaling performed for the acquisition function.

A comparison between the terms for acquisition function in (25) and the ones in (17) is depicted in Figure 6. As the number of samples increases, $z(\mathbf{x})$ gets progressively smaller (see Section 4.1) and simply dividing $\hat{f}(\mathbf{x})$ by $\Delta \hat{F}(\mathcal{X})$ as in (17) is not enough to make the exploration and exploitation contributions comparable. Thus, unless δ in (17) is dynamically varied in between iterations, solving Problem (8) with $a(\mathbf{x})$ in (17) becomes similar to performing pure exploitation. This, in turn, can lead GLISp [3] to get stuck on a local minima of Problem (3) with no way of escaping (especially if the surrogate model is not expressive enough to capture the location of the global minimizer). Viceversa,

by performing min-max rescaling as proposed in (25), the exploitation and exploration contributions stay comparable throughout the procedure and approximately assume the same range. For this reason, it is also more straightforward to define δ in (25) compared to the one in (17).

From Theorems 2 and 3, we can immediately deduce the following results on the differentiability of $a(\mathbf{x})$ in (25).

Theorem 4. *The acquisition function $a(\mathbf{x})$ in (25) is differentiable everywhere provided that the chosen surrogate function $\hat{f}(\mathbf{x})$ is differentiable everywhere.*

Lemma 3. *The gradient of the acquisition function $a(\mathbf{x})$ in (25) is*

$$\nabla_{\mathbf{x}} a(\mathbf{x}) = \frac{\delta}{\Delta \hat{F}(\mathcal{X}_{aug})} \cdot \nabla_{\mathbf{x}} \hat{f}(\mathbf{x}) + \frac{1 - \delta}{\Delta Z(\mathcal{X}_{aug})} \cdot \nabla_{\mathbf{x}} z(\mathbf{x}). \quad (26)$$

Recall that, at each iteration, we find the next sample to try, \mathbf{x}_{N+1} , by solving Problem (8). It is possible to use derivative-based optimization solvers since $a(\mathbf{x})$ is differentiable everywhere. In general, the acquisition function is *multimodal* and thus it is better to employ a global optimization procedure. Moreover, $a(\mathbf{x})$ is cheap to evaluate, therefore we are not particularly concerned on its number of function evaluations.

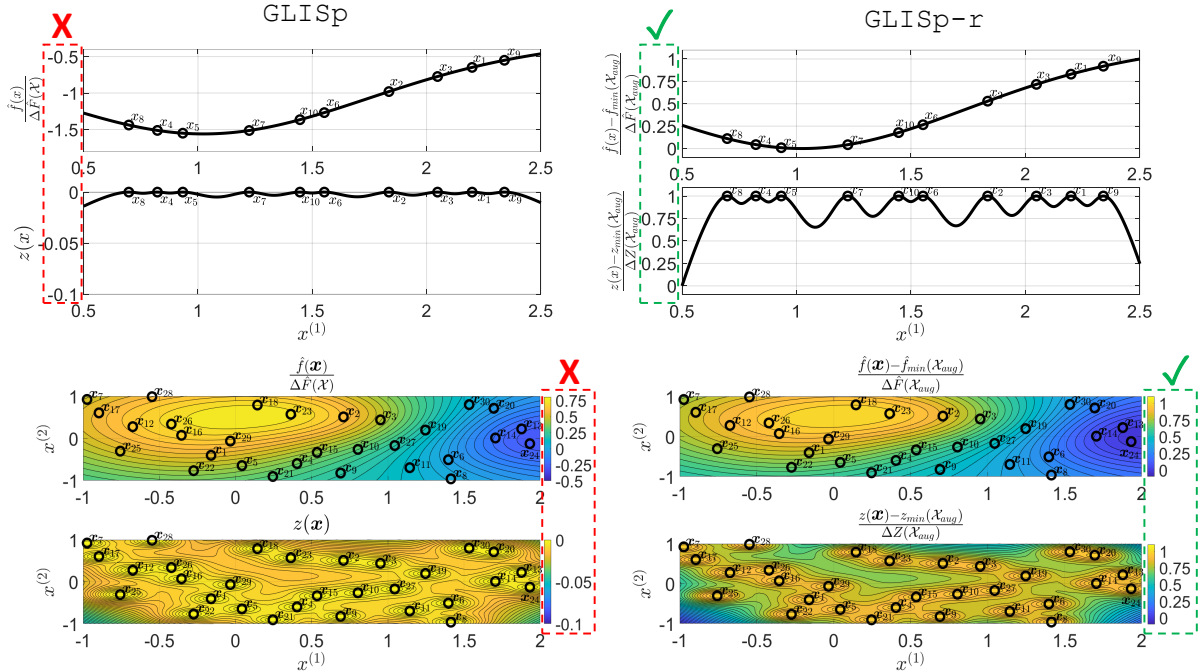


Figure 6: Comparison between the terms in acquisition functions (17) (left) and (25) (right). The top row is obtained by using the one-dimensional gramacy and lee [14] function as $f(\mathbf{x})$ and $N = 10$, while the bottom row is achieved from the two-dimensional adjiman [17] function and $N = 30$. The number of clusters used to build \mathcal{X}_{aug} through Algorithm 1 is $K_{aug} = 5$. In both cases, notice how, for GLISp [2], the exploration function $z(\mathbf{x})$ is not comparable with the rescaled surrogate $\frac{\hat{f}(\mathbf{x})}{\Delta \hat{F}(\mathcal{X})}$ since it assumes values that are one or two orders of magnitude lower.

4.3 Greedy δ -cycling

Many black-box optimization algorithms explicitly vary the exploration-exploitation trade-off in between the iterations of the procedure. Just to cite a few:

- Gutmann-RBF [15] uses an acquisition function that is a measure of “bumpiness” of the RBF surrogate which depends upon a target value t to aim for. The author suggests to cycle the values of t between $t = \min_{\mathbf{x} \in \Omega} \hat{f}(\mathbf{x})$ (local search) and $t = -\infty$ (global search).

- The authors of MSRS [26], which uses an acquisition function that is similar to (25), propose to cycle between different values of δ as to prioritize exploration or exploitation more.
- In algorithm SO-SA [33], which is a revisit of MSRS [26], the weight δ is chosen in a random fashion at each iteration. Moreover, the authors adopt a greedy strategy, i.e. the trade-off is kept unaltered until it fails to find a significantly better solution.

In the original formulations of GLISp [3], hyperparameter δ is kept constant throughout the whole optimization procedure. Also, defining some form of cycling for such coefficient used in acquisition function (17) can be quite complex given that, as previously seen, the additive terms are not always comparable. In this work, we propose a strategy that is in between MSRS [26] and SO-SA [33], which we will refer to as *greedy δ -cycling*. In particular, we define a set of $N_{cycle} \geq 1$ weights to cycle:

$$\Delta_{cycle} = \{\delta_0, \dots, \delta_{N_{cycle}-1}\}. \quad (27)$$

Δ_{cycle} should contain values that are well spread within the $[0, 1]$ range as to properly alternate between local and global search. Greedy δ -cycling operates as follows: suppose that, at iteration k , we have at our disposal $|\mathcal{X}| = N$ samples and denote the trade-off parameter δ in (25) as $\delta(k)$ to highlight the iteration number. Furthermore, assume $\delta(k) = \delta_j \in \Delta_{cycle}$, which is used to find the new candidate sample \mathbf{x}_{N+1} at iteration k by solving Problem (8). Then, if $\mathbf{x}_{N+1} \succ \mathbf{x}_{best}(N)$ (i.e., there has been some improvement), the trade-off is kept unchanged, $\delta(k+1) = \delta(k) = \delta_j$. Otherwise, we cycle the values in Δ_{cycle} , obtaining $\delta(k+1) = \delta_{(j+1) \bmod N_{cycle}}$. Thus:

$$\delta(k+1) = \begin{cases} \delta_j & \text{If } \mathbf{x}_{N+1} \succ \mathbf{x}_{best}(N) \\ \delta_{(j+1) \bmod N_{cycle}} & \text{If } \mathbf{x}_{best}(N) \succsim \mathbf{x}_{N+1} \end{cases}$$

In Section 5, we will discuss the choice of the cycling set more in detail and also cover its relationship with the convergence of GLISp-r.

5 Algorithm GLISp-r and convergence

Algorithm 3 describes each step of GLISp-r. The procedure follows a typical surrogate-based optimization scheme [32]. Differently from GLISp [3], GLISp-r requires building the augmented sample set and uses the acquisition function in (25) instead of the one in (17). We can summarize the algorithm as follows:

1. First of all, the decision variable \mathbf{x} (and, consequently, the optimization problem in (3)) is rescaled using the method proposed in [3].
2. Then, there is an experimental design phase which generates an initial set of samples \mathcal{X} , $|\mathcal{X}| = N$. Similarly to GLISp [3], we use a Latin Hypercube Design (LHD) [22].
3. After that, we let the human decision-maker express preferences between the samples in \mathcal{X} . The comparisons are driven by employing the transitive property of the preference relation \succsim (Section 2), so that it is possible to obtain the initial best sample $\mathbf{x}_{best}(N)$. See Algorithm 2 for more details.
4. Iteratively, until the budget N_{max} is exhausted:
 - (a) (Possibly) recalibrate the shape parameter ϵ of the surrogate model in (10) using grid-search Leave One Out Cross-validation (LOOCV) as proposed in [3]. In practice, the recalibration is not performed at every iteration but only at certain ones, as specified by a set \mathcal{I}_{CV} ;
 - (b) Build surrogate model in (10) with β found by solving Problem (13);
 - (c) Build the augmented sample set \mathcal{X}_{aug} using Algorithm 1;
 - (d) Find the next candidate sample \mathbf{x}_{N+1} by solving Problem (8), with δ in (25) selected using the strategy in Section 4.3;
 - (e) Let the user express a preference between the new candidate sample \mathbf{x}_{N+1} and the best one found so far $\mathbf{x}_{best}(N)$;
 - (f) Update the data.

5.1 Convergence of GLISp-r

Whenever we are dealing with any global optimization algorithm, it is possible to guarantee its convergence to the global minimizer of Problem (3) by proving the following Theorem.

Algorithm 2 Initial queries for GLISp-r**Input:**

- (i) Initial set of samples \mathcal{X} , $|\mathcal{X}| = N$, in (5).

Output:

- (i) Set of preferences \mathcal{B} in (6),
- (ii) Mapping set \mathcal{S} in (7),
- (iii) Initial best sample $\mathbf{x}_{best}(N)$.

```

1: Initialize the best sample as  $\mathbf{x}_{best}(1) = \mathbf{x}_1, i_{best} = 1$ 
2: Initialize the sets  $\mathcal{B} = \emptyset$  and  $\mathcal{S} = \emptyset$ 
3: for  $i = 2$  to  $|\mathcal{X}| = N$  do
4:   Express preference between  $\mathbf{x}_{best}(i-1)$  and  $\mathbf{x}_i$ , obtaining  $b = \pi(\mathbf{x}_{best}(i-1), \mathbf{x}_i)$ 
5:   Update sets  $\mathcal{B}$  and  $\mathcal{S}$ :  $\mathcal{B} = \mathcal{B} \cup \{b\}$  and  $\mathcal{S} = \mathcal{S} \cup \{(i_{best}, i)\}$ 
6:   if  $b = 1$  (i.e.  $\mathbf{x}_i \succ \mathbf{x}_{best}(i-1)$ ) then
7:     Update the best,  $\mathbf{x}_{best}(i) = \mathbf{x}_i$  and  $i_{best} = i$ 
8:   else
9:     Keep best unaltered,  $\mathbf{x}_{best}(i) = \mathbf{x}_{best}(i-1)$ 

```

Theorem 5 (Convergence of a global optimization algorithm [29]). *Consider the global optimization problem in (3). Let $\Omega \subset \mathbb{R}^n$ be a compact set and $f : \mathbb{R}^n \rightarrow \mathbb{R}$ be a continuous function. Then, an algorithm converges to the global minimum of every continuous function on Ω if and only if its sequence of iterates,*

$$\langle \mathbf{x}_i \rangle_{i \geq 1} = \langle \mathbf{x}_1, \mathbf{x}_2, \dots \rangle,$$

is everywhere dense in Ω .

In the preference-based framework, we need to ensure that the scoring function $f(\mathbf{x})$ that represents the preference relation \succsim is continuous. Theorem 1 gives us necessary conditions on \succsim to achieve such property. Furthermore, Proposition 1 can be used to assure the existence of a \succsim -maximum in Ω . We can state the following Theorem, whose proof is provided in Appendix A.

Theorem 6 (Convergence of GLISp-r). *Let \succsim be a continuous and complete preference relation and $\Omega \subset \mathbb{R}^n$ be a compact set. Then, provided that there $\exists \delta_j \in \Delta_{cycle}$ such that $\delta_j = 0$ and $N_{max} \rightarrow \infty$, GLISp-r converges to the global minimizer of Problem (3) for any set of initial points \mathcal{X} , $|\mathcal{X}| = N$, as well as any choice of its remaining hyperparameters.*

Remark 2. *Theorem 6 guarantees that, under some hypotheses, GLISp-r converges to the \succsim -maximum of Ω , however it does not give any indication on the convergence rate. In particular, if Δ_{cycle} is actually $\{0\}$, GLISp-r is equivalent to performing exhaustive search [1], which is quite inefficient. Therefore, it is best to include some $\delta_j \in \Delta_{cycle}$ which allow the surrogate model to be taken into consideration. For this reason, we suggest to include terms that are well spread within the $[0, 1]$ range, including a zero entry to ensure the result of Theorem 6. Intuitively, the rate of convergence will be dependent on how well $\hat{f}(\mathbf{x})$ approximates $f(\mathbf{x})$ as well as on the choice of Δ_{cycle} .*

6 Numerical results

In this Section we are going to compare the performances of algorithms GLISp-r and GLISp [3] on a variety of benchmark global optimization problems [14, 17], reported in Table 1. We also consider a different version of the IDW distance function in (15), which has been proposed in [36] by the same authors:

$$z(\mathbf{x}) = \left(1 - \frac{N}{N_{max}}\right) \cdot \arctan\left(\frac{\sum_{i=1}^N w_i(\mathbf{x}_{best}(N))}{\sum_{i=1}^N w_i(\mathbf{x})}\right) + \frac{N}{N_{max}} \cdot \arctan\left(\frac{1}{\sum_{i=1}^N w_i(\mathbf{x})}\right). \quad (28)$$

Algorithm 3 GLISp-r algorithm**Input:**

- (i) Constraint set Ω in (1),
- (ii) Initial number of samples $N \geq 2$,
- (iii) Budget $N_{max} > N$,
- (iv) Hyperparameters for surrogate model (10) (and (12)), namely shape parameter $\epsilon \in \mathbb{R}_{>0}$, radial function $\varphi(\cdot)$, regularization parameter $\lambda \in \mathbb{R}_{\geq 0}$ and tolerance $\sigma \in \mathbb{R}_{>0}$,
- (v) Number of clusters K_{aug} for the augmented sample set \mathcal{X}_{aug} (Section 4.1),
- (vi) Possible shape parameters for grid-search LOOCV: $\epsilon_{grid} = \{\epsilon_1, \dots, \epsilon_{N_{models}}\}$, $\epsilon_m \in \mathbb{R}_{>0}, \forall m = 1, \dots, N_{models}$ and $\epsilon \in \epsilon_{grid}$,
- (vii) Set of indexes for recalibration of the surrogate model $\mathcal{I}_{CV} \subseteq \{N, N+1, \dots, N_{max}\}$,
- (viii) Exploration-exploitation trade-off cycle Δ_{cycle} (Section 4.3.).

Output:

- (i) Best sample obtained by the procedure $\mathbf{x}_{best}(N_{max})$.

```

1: Rescale Problem (3) as done in GLISp [3]
2: Select a set of starting points  $\mathcal{X}$ ,  $|\mathcal{X}| = N$ , using a Latin Hypercube Design [32]
3: Evaluate the samples in  $\mathcal{X}$ , using Algorithm 2, obtaining  $\mathcal{B}$ ,  $\mathcal{S}$  and  $\mathbf{x}_{best}(N)$ 
4: for  $k = 1, 2, \dots, N_{max} - |\mathcal{X}|$  do
5:   if  $k \in \mathcal{I}_{CV}$  then
6:     Recalibrate the shape parameter  $\epsilon$  of model (10) as proposed in GLISp [3]
7:     Build surrogate model  $\hat{f}(\mathbf{x})$  from  $\mathcal{X}, \mathcal{B}, \mathcal{S}$  by solving Problem (13)
8:     Build the augmented sample set  $\mathcal{X}_{aug}$  using Algorithm 1
9:     Select  $\delta$  for the current iteration from  $\Delta_{cycle}$  (Section 4.3)
10:    Solve Problem (8) to obtain the new candidate sample  $\mathbf{x}_{N+1}$ 
11:    Let the human decision-maker express preference  $b_{M+1} = \pi(\mathbf{x}_{N+1}, \mathbf{x}_{best}(N))$ 
12:    if  $b_{M+1} = -1$  (i.e. the new candidate sample is preferred to the best one found so far) then
13:      Set  $\mathbf{x}_{best}(N+1) = \mathbf{x}_{N+1}$ 
14:    else
15:      Set  $\mathbf{x}_{best}(N+1) = \mathbf{x}_{best}(N)$  (no improvement)
16:    Update the set of samples  $\mathcal{X}$ , preferences  $\mathcal{B}$  and mapping set  $\mathcal{S}$ .
17:    Set  $N = N + 1, M = M + 1$ 

```

This definition of $z(\mathbf{x})$ also aims to address the shortcomings of Function (15) (analyzed in Section 3.2) which can cause GLISp [3] to get stuck on a local minima with no way of escaping. We will refer to the algorithm that uses IDW distance function in (28) as C-GLISp (as it is named in [36]).

GLISp-r has been implemented in MATLAB. Similarly, we have used the MATLAB code for GLISp provided in [3] (formally, version 2.4 of the software package) and the one for C-GLISp supplied in [36] (version 3.0 of the same code package). For all the procedures, Problem (8) has been solved using Particle Swarm Optimization (PSWARM). In particular, we have used its MATLAB implementation provided by [30, 31, 20].

In order to achieve a fair comparison, we have chosen the same hyperparameters for both GLISp/C-GLISp [3, 36] and GLISp-r, whenever possible. This applies, for example, to the shape parameter ϵ and the radial function $\varphi(\cdot)$. Viceversa, for those hyperparameters that are defined differently, such as δ , we have used the settings suggested by

name	n	$f(\mathbf{x})$	l	u	Global minimizer \mathbf{x}^*	$f(\mathbf{x}^*)$
bempeard	1	$\left[1 + \frac{x^{(1)} \cdot \sin(2 \cdot x^{(1)}) \cdot \cos(3 \cdot x^{(1)})}{1 + (x^{(1)})^2}\right]^2 + \frac{(x^{(1)})^2}{12} + \frac{x^{(1)}}{10}$	-3	3	-0.9599	0.2795
gramacy and lee	1	$\frac{\sin(10 \cdot \pi \cdot x^{(1)})}{2 \cdot x^{(1)}} + (x^{(1)} - 1)^4$	0.5	2.5	0.5486	-0.8690
ackley	2	$-20 \cdot e^{-0.02 \sqrt{n-1} \cdot \sum_{i=1}^n (x^{(i)})^2} - e^{n-1} \sum_{i=1}^n \cos(2 \cdot \pi \cdot x^{(i)}) + 20 + e$	$-35 \cdot \mathbf{1}_n$	$35 \cdot \mathbf{1}_n$	$\mathbf{0}_n$	0
bukin 6	2	$100 \cdot \sqrt{\ x^{(2)} - 0.01 \cdot (x^{(1)})^2\ _2} + 0.01 \cdot \ x^{(1)} + 10\ _2$	$\begin{bmatrix} -15 \\ -5 \end{bmatrix}$	$\begin{bmatrix} -5 \\ 3 \end{bmatrix}$	$\begin{bmatrix} -10 \\ 1 \end{bmatrix}$	0
levi 13	2	$\sin(3 \cdot \pi \cdot x^{(1)})^2 + (x^{(1)} - 1)^2 \cdot [1 + \sin(3 \cdot \pi \cdot x^{(2)})^2] + (x^{(2)} - 1)^2 \cdot [1 + \sin(2 \cdot \pi \cdot x^{(2)})^2]$	$-10 \cdot \mathbf{1}_n$	$10 \cdot \mathbf{1}_n$	$\mathbf{1}_n$	0
adjiman	2	$\cos(x^{(1)}) \cdot \sin(x^{(2)}) - \frac{x^{(1)}}{(x^{(2)})^2 + 1}$	$\begin{bmatrix} -1 \\ -1 \end{bmatrix}$	$\begin{bmatrix} 2 \\ 1 \end{bmatrix}$	$\begin{bmatrix} 2 \\ 0.10578 \end{bmatrix}$	-2.02181
camel three hump	2	$2 \cdot (x^{(1)})^2 - 1.05 \cdot (x^{(1)})^4 + \frac{(x^{(1)})^6}{6} + x^{(1)} \cdot x^{(2)} + (x^{(2)})^2$	$-5 \cdot \mathbf{1}_n$	$5 \cdot \mathbf{1}_n$	$\mathbf{0}_n$	0
rosenbrock	5	$\sum_{i=1}^{n-1} \left\{ 100 \cdot [x^{(i+1)} - (x^{(i)})^2]^2 + [x^{(i)} - 1]^2 \right\}$	$-30 \cdot \mathbf{1}_n$	$30 \cdot \mathbf{1}_n$	$\mathbf{1}_n$	0
step 2	5	$\sum_{i=1}^n [x^{(i)} + 0.5]^2$	$-100 \cdot \mathbf{1}_n$	$100 \cdot \mathbf{1}_n$	$-0.5 \cdot \mathbf{1}_n$	0
salomon	5	$1 - \cos\left[2 \cdot \pi \cdot \sqrt{\sum_{i=1}^n (x^{(i)})^2}\right] + 0.1 \cdot \sqrt{\sum_{i=1}^n (x^{(i)})^2}$	$-100 \cdot \mathbf{1}_n$	$100 \cdot \mathbf{1}_n$	$\mathbf{0}_n$	0

Table 1: Considered benchmark optimization problems. These functions are taken from [2, 14, 17].

	GLISp [3] and C-GLISp [36]	GLISp-r
Number of initial samples N	$4 \cdot n$	
Radial function $\varphi(\cdot)$	inverse quadratic	
Shape parameter ϵ	1	
Regularization parameter λ	10^{-6}	
Tolerance σ	10^{-2}	
Exploration-exploitation trade-off δ or Δ_{cycle}	2	{0.95, 0.7, 0.35, 0}
Recalibration indexes \mathcal{I}_{CV}	{1, 50, 100}	
Grid of ϵ for cross-validation	{0.1000, 0.1668, 0.2783, 0.4642, 0.7743, 1.0000, 1.2915, 2.1544, 3.5938, 5.9948, 10}	
Number of centroids K_{aug}	not defined	5
Budget N_{max}	200	

Table 2: Settings of the algorithms used to solve the benchmark optimization problems.

the authors. Regarding GLISp-r, we have chosen $\Delta_{cycle} = \{0.95, 0.7, 0.35, 0\}$, where we have included a zero term to comply with the convergence result in Theorem 6. The reasoning behind this cycling set is that, after the initial sampling phase, we give priority to the surrogate as to drive the algorithm towards more promising regions of the domain, for example where local minima are located. In practice, if $f(\mathbf{x})$ is a function that can be well approximated by $\hat{f}(\mathbf{x})$ with very few samples, starting with a δ that is close to 1 might lead the procedure to converge quite faster. If that is not the case, the remaining terms contained inside Δ_{cycle} promote the exploration of other zones of the constraint set Ω , either dependently or independently from $\hat{f}(\mathbf{x})$. Lastly, we use $K_{aug} = 5$ for all optimization problems since, empirically, it has proven to be good enough to rescale $z(\mathbf{x})$ and $\hat{f}(\mathbf{x})$ in most cases. All the settings of the algorithms are reported in Table 2.

We run the procedures using a fixed budget of samples $N_{max} = 200$ and perform $N_{MC} = 100$ Monte Carlo simulations, starting from different points. The preferences between couples of samples are expressed using the preference function in (4). We compare the procedures both from a visual standpoint, i.e. by depicting the best, median and worst case performances in Figure 7, and by using some indicators. In particular, we report the *number of samples required to reach a certain accuracy* [1], $N_{acc>t}$, which is defined as:

$$acc(N) = \frac{f(\mathbf{x}_{best}(N)) - f(\mathbf{x}_1)}{f(\mathbf{x}^*) - f(\mathbf{x}_1)} \cdot 100, \quad (29)$$

$$N_{acc>t} = N : acc(N) > t,$$

where t is a threshold, $0\% \leq t \leq 100\%$. In our simulations we consider $t = 95\%$ and $t = 99\%$. We also report an additional indicator, $d_{rel}(N_{max})$, which corresponds to the *relative distance from the global minimizer at the last iteration of the procedure*:

$$d_{rel}(N_{max}) = \frac{\|\mathbf{x}_{best}(N_{max}) - \mathbf{x}^*\|_2}{\|\mathbf{u} - \mathbf{l}\|_2} \cdot 100. \tag{30}$$

Note that, differently from $acc(N)$, this indicator is not monotone and therefore it only makes sense to evaluate it when the budget is exhausted. The performances achieved by the procedures in the median case are reported in Table 3.

$f(x)$	$N_{acc>95\%}$			$N_{acc>99\%}$			$d_{rel}(N_{max})$		
	GLISp [3]	C-GLISp [36]	GLISp-r	GLISp [3]	C-GLISp [36]	GLISp-r	GLISp [3]	C-GLISp [36]	GLISp-r
bemporad	10	16	11	12	26	14	0.00%	0.02%	0.03%
gramacy and lee	n.r.	31	33	n.r.	66	41	15.01%	0.03%	0.01%
ackley	n.r.	n.r.	n.r.	n.r.	n.r.	n.r.	4.03%	2.08%	2.25%
bukin 6	25	161	77	78	n.r.	n.r.	17.47%	17.55%	15.32%
levi 13	10	20	10	15	78	21	0.60%	0.68%	0.40%
adjiman	12	13	13	13	25	17	0.00%	0.09%	0.00%
camel three hump	8	8	9	13	54	16	0.01%	0.21%	0.03%
rosenbrock	21	22	21	22	59	22	1.71%	3.78%	3.50%
step 2	22	106	22	32	177	45	0.29%	0.79%	0.34%
salomon	n.r.	n.r.	n.r.	n.r.	n.r.	n.r.	2.85%	2.20%	3.74%

Table 3: Performance indicators for the considered algorithms. All these metrics have been computed only for the median case. The lowest value among the algorithms (best performance) is highlighted using a bold font. The acronym n.r. stands for “not reached” and remarks the situations for which the procedure is not able to reach a certain accuracy within the fixed budget.

From these simulations we gather that the median performances of GLISp [3] are often slightly better than GLISp-r or at least comparable. However, the former procedure is more likely to get stuck on some local minima of $f(x)$ with no way of escaping, as highlighted by the worst cases of most benchmark functions in Figure 7. An extreme case is the gramacy and lee function, for which GLISp [3] fails to achieve a satisfactory median-wise accuracy. Viceversa, the rate of convergence of C-GLISp [36] is quite often worse than the other two algorithms. However, it is important to note that both C-GLISp [36] and GLISp-r are more consistent in finding the global minimizers of the benchmark functions. Figure 8 depicts $\mathbf{x}_{best}(N_{max})$ for all 100 simulations with the gramacy and lee function and corresponding to the three algorithms. In this case, $f(x)$ is a multimodal function and GLISp [3] gets stuck at a local minima on several simulations. Viceversa, C-GLISp [36] and GLISp-r find the global minimizer more reliably.

7 Summary and discussion

In this paper, we proposed a more robust version of algorithm GLISp [3]. The proposed algorithm is less likely to get stuck on the local minimizers of the scoring function. To do so, we have addressed some limitations concerning the exploration function $z(x)$ in (15), defined a new acquisition function and proposed to dynamically vary the exploration-exploitation trade-off using the greedy δ -cycling strategy. Many black-box optimization algorithms follow this rationale of alternating between local and global search by varying the trade-off parameter, however no such strategy has been employed in GLISp [3]. Furthermore, using notions of utility theory, we have been able to prove the convergence of GLISp-r, which is strictly related to the choice of the cycling set Δ_{cycle} .

Numerical results show that GLISp-r can be slightly slower (i.e. it requires more samples to converge to the global minimizer of Problem (3)) than GLISp [3] but is more consistent in finding the global solution of Problem (3). Moreover, we have also considered algorithm C-GLISp [36], proposed by the same authors, which overcomes the limitations of $z(x)$ in (15) by defining a different version of the exploration function. In our simulations, we have observed that,

even though C-GLISp [36] is less likely to get stuck on local minima, it often exhibits slower convergence rates compared to GLISp [3] and GLISp-r.

Further research is devoted to extending GLISp-r in order to also handle black-box constraints. One possibility is to follow the same reasoning behind C-GLISp⁴ [36], which does so by adding a term to the acquisition function that penalizes exploration in those zones where the black-box constraints are likely to be violated.

References

- [1] Charles Audet and Warren Hare. *Derivative-free and blackbox optimization*. Springer, 2017.
- [2] Alberto Bemporad. Global optimization via inverse distance weighting and radial basis functions. *Computational Optimization and Applications*, 77(2):571–595, Nov 2020.
- [3] Alberto Bemporad and Dario Piga. Global optimization based on active preference learning with radial basis functions. *Machine Learning*, 110(2):417–448, Feb 2021.
- [4] Alessio Benavoli, Dario Azzimonti, and Dario Piga. Preferential bayesian optimisation with skew gaussian processes. In *Proceedings of the Genetic and Evolutionary Computation Conference Companion*, pages 1842–1850, 2021.
- [5] Christopher M Bishop. *Pattern recognition*, volume 128. 2006.
- [6] Eric Brochu, Nando De Freitas, and Abhijeet Ghosh. Active preference learning with discrete choice data. In *NIPS*, pages 409–416, 2007.
- [7] Wei Chu and Zoubin Ghahramani. Preference learning with gaussian processes. *Proceedings of the 22nd international conference on Machine learning*, pages 137–144, 2005.
- [8] Gerard Debreu. *Theory of value: An axiomatic analysis of economic equilibrium*, volume 17. Yale University Press, 1959.
- [9] Gregory E Fasshauer. *Meshfree approximation methods with MATLAB*, volume 6. World Scientific, 2007.
- [10] Bengt Fornberg and Natasha Flyer. *A primer on radial basis functions with applications to the geosciences*. SIAM, 2015.
- [11] Jerome Friedman, Trevor Hastie, Robert Tibshirani, et al. *The elements of statistical learning*, volume 1. Springer series in statistics New York, 2001.
- [12] Johannes Fürnkranz and Eyke Hüllermeier. *Preference learning and ranking by pairwise comparison*. Springer, 2010.
- [13] Javier González, Zhenwen Dai, Andreas Damianou, and Neil D Lawrence. Preferential bayesian optimization. In *International Conference on Machine Learning*, pages 1282–1291. PMLR, 2017.
- [14] Robert B Gramacy and Herbert KH Lee. Cases for the nugget in modeling computer experiments. *Statistics and Computing*, 22(3):713–722, 2012.
- [15] H-M Gutmann. A radial basis function method for global optimization. *Journal of global optimization*, 19(3):201–227, 2001.
- [16] Jiawei Han, Jian Pei, and Micheline Kamber. *Data mining: concepts and techniques*. Elsevier, 2011.
- [17] Momin Jamil and Xin-She Yang. A literature survey of benchmark functions for global optimisation problems. *International Journal of Mathematical Modelling and Numerical Optimisation*, 4(2):150–194, 2013.
- [18] Donald R Jones. A taxonomy of global optimization methods based on response surfaces. *Journal of global optimization*, 21(4):345–383, 2001.
- [19] John L Kelley. *General topology*. Courier Dover Publications, 2017.
- [20] Hoai A Le Thi, A Ismael F Vaz, and LN Vicente. Optimizing radial basis functions by dc programming and its use in direct search for global derivative-free optimization. *Top*, 20(1):190–214, 2012.
- [21] Rafael Martí, Jose A. Lozano, Alexander Mendiburu, and Leticia Hernando. *Multi-start Methods*, pages 155–175. Springer International Publishing, Cham, 2018.

⁴Note that, in this paper, we have used C-GLISp [36] only to test how the IDW distance function in (28) compares with the other formulation in (15). However, C-GLISp [36] has been developed mainly to extend GLISp [3] in order to handle black-box constraints. The different definition of $z(\mathbf{x})$ is only a minor detail of such paper.

- [22] Michael D McKay, Richard J Beckman, and William J Conover. A comparison of three methods for selecting values of input variables in the analysis of output from a computer code. *Technometrics*, 42(1):55–61, 2000.
- [23] Jorge Nocedal and Stephen Wright. *Numerical optimization*. Springer Science & Business Media, 2006.
- [24] Efe A Ok. *Real analysis with economic applications*. Princeton University Press, 2011.
- [25] Rommel G. Regis and Christine A. Shoemaker. Constrained global optimization of expensive black box functions using radial basis functions. *Journal of Global optimization*, 31(1):153–171, 2005.
- [26] Rommel G. Regis and Christine A. Shoemaker. A stochastic radial basis function method for the global optimization of expensive functions. *INFORMS Journal on Computing*, 19(4):497–509, November 2007.
- [27] Loris Roveda, Beatrice Maggioni, Elia Maresscotti, Asad Ali Shahid, Andrea Maria Zanchettin, Alberto Bemporad, and Dario Piga. Pairwise preferences-based optimization of a path-based velocity planner in robotic sealing tasks. *IEEE Robotics and Automation Letters*, 6(4):6632–6639, 2021.
- [28] Donald Shepard. A two-dimensional interpolation function for irregularly-spaced data. In *Proceedings of the 1968 23rd ACM national conference*, pages 517–524, 1968.
- [29] Aimo Torn and Antanas Zilinskas. *Global Optimization*. Lecture Notes in Computer Science, 1989.
- [30] A Ismael F Vaz and Luis N Vicente. A particle swarm pattern search method for bound constrained global optimization. *Journal of Global Optimization*, 39(2):197–219, 2007.
- [31] A Ismael F Vaz and Luis Nunes Vicente. Pswarm: a hybrid solver for linearly constrained global derivative-free optimization. *Optimization Methods & Software*, 24(4-5):669–685, 2009.
- [32] Ky Khac Vu, Claudia d’Ambrosio, Youssef Hamadi, and Leo Liberti. Surrogate-based methods for black-box optimization. *International Transactions in Operational Research*, 24(3):393–424, 2017.
- [33] Yilun Wang and Christine A Shoemaker. A general stochastic algorithmic framework for minimizing expensive black box objective functions based on surrogate models and sensitivity analysis. *arXiv preprint arXiv:1410.6271*, 2014.
- [34] Christopher K Williams and Carl Edward Rasmussen. *Gaussian processes for machine learning*, volume 2. MIT press Cambridge, MA, 2006.
- [35] Mengjia Zhu, Alberto Bemporad, and Dario Piga. Preference-based mpc calibration. *arXiv preprint arXiv:2003.11294*, 2020.
- [36] Mengjia Zhu, Dario Piga, and Alberto Bemporad. C-glisip: Preference-based global optimization under unknown constraints with applications to controller calibration, 2021.

A Proofs

Proof of Lemma 2 The gradient of the IDW distance function in (15), $\nabla_{\mathbf{x}} z(\mathbf{x})$, is defined $\forall \mathbf{x} \in \mathbb{R}^n$ (see Theorem 3 which has been proven in [2]) and can be computed by repeatedly applying the chain rule. First of all, it is easy to prove that any Inverse Distance Weighting function $w_i(\mathbf{x})$ in (14) is differentiable $\forall \mathbf{x} \in \mathbb{R}^n \setminus \{\mathbf{x}_i\}$. That is because the squared Euclidean norm $\|\mathbf{x} - \mathbf{x}_i\|_2^2$ is differentiable everywhere and also

$$\|\mathbf{x} - \mathbf{x}_i\|_2^2 \neq 0, \forall \mathbf{x} \in \mathbb{R}^n \setminus \{\mathbf{x}_i\}.$$

Therefore, for the reciprocal rule, $w_i(\mathbf{x})$ is differentiable $\forall \mathbf{x} \in \mathbb{R}^n \setminus \{\mathbf{x}_i\}$. In order to compute the gradient of $w_i(\mathbf{x})$ in (14), recall that the gradient of the squared Euclidean norm is equal to:

$$\nabla_{\mathbf{x}} \|\mathbf{x} - \mathbf{x}_i\|_2^2 = 2 \cdot (\mathbf{x} - \mathbf{x}_i). \quad (31)$$

Consider the domain $\mathbf{x} \in \mathbb{R}^n \setminus \{\mathbf{x}_i\}$, then it is easy to prove, using (31), that:

$$\begin{aligned} \nabla_{\mathbf{x}} w_i(\mathbf{x}) &= -2 \cdot \frac{\mathbf{x} - \mathbf{x}_i}{\|\mathbf{x} - \mathbf{x}_i\|_2^4} \\ &= -2 \cdot (\mathbf{x} - \mathbf{x}_i) \cdot w_i(\mathbf{x})^2, \forall \mathbf{x} \in \mathbb{R}^n \setminus \{\mathbf{x}_i\}. \end{aligned} \quad (32)$$

Now, let us focus on the argument of the arctan (\cdot) function in $z(\mathbf{x})$, which is (see (15)):

$$h(\mathbf{x}) = \frac{1}{\sum_{i=1}^N w_i(\mathbf{x})}, \forall \mathbf{x} \in \mathbb{R}^n \setminus \mathcal{X}.$$

It is possible to compute the gradient of $h(\mathbf{x})$ using the chain rule in combination with (32):

$$\nabla_{\mathbf{x}} h(\mathbf{x}) = 2 \cdot \frac{\sum_{i=1}^N (\mathbf{x} - \mathbf{x}_i) \cdot w_i(\mathbf{x})^2}{\left[\sum_{i=1}^N w_i(\mathbf{x})\right]^2}, \forall \mathbf{x} \in \mathbb{R}^n \setminus \mathcal{X}. \quad (33)$$

Finally, using (33) and applying the chain rule one last time, we can compute the gradient of the IDW distance function in (15):

$$\begin{aligned} \nabla_{\mathbf{x}} z(\mathbf{x}) &= -\frac{4}{\pi} \cdot \frac{1}{1 + \left[\frac{1}{\sum_{i=1}^N w_i(\mathbf{x})}\right]^2} \cdot \frac{\sum_{i=1}^N (\mathbf{x} - \mathbf{x}_i) \cdot w_i(\mathbf{x})^2}{\left[\sum_{i=1}^N w_i(\mathbf{x})\right]^2} \\ &= -\frac{4}{\pi} \cdot \frac{\sum_{i=1}^N (\mathbf{x} - \mathbf{x}_i) \cdot w_i(\mathbf{x})^2}{1 + \left[\sum_{i=1}^N w_i(\mathbf{x})\right]^2}, \forall \mathbf{x} \in \mathbb{R}^n \setminus \mathcal{X}. \end{aligned} \quad (34)$$

Now, let us consider the case $\mathbf{x}_i \in \mathcal{X}$. In [2], the authors have proven that all partial derivatives of $z(\mathbf{x})$ in (15) are zero at $\mathbf{x}_i \in \mathcal{X}$, i.e.

$$\nabla_{\mathbf{x}} z(\mathbf{x}_i) = \mathbf{0}_n, \forall \mathbf{x}_i \in \mathcal{X}. \quad (35)$$

Lastly, combining (34) and (35), we obtain the expression for the gradient of the IDW distance function $\forall \mathbf{x} \in \mathbb{R}^n$, as reported in (16). \square

Proof of Proposition 2 Recall that:

- (i) By definition, $z : \mathbb{R}^n \rightarrow (-1, 0]$,
- (ii) $\nabla_{\mathbf{x}} z(\mathbf{x}_i) = \mathbf{0}_n, \forall \mathbf{x}_i \in \mathcal{X}$ (see (16)),
- (iii) $z(\mathbf{x}) = -\frac{2}{\pi} \cdot \arctan\left(\frac{1}{\sum_{i=1}^N w_i(\mathbf{x})}\right) < 0, \forall \mathbf{x} \notin \mathcal{X}$ (see (15)),
- (iv) $z(\mathbf{x}_i) = 0, \forall \mathbf{x}_i \in \mathcal{X}$ (see (15)).

From (ii) we deduce that $\forall \mathbf{x}_i \in \mathcal{X}$ are stationary points for $z(\mathbf{x})$. Point (iii), in conjunction with (iv), imply that such samples are local maximizers of the IDW distance function in (15) since there exists a neighborhood $\mathcal{N}_{\mathbf{x}_i}$ of \mathbf{x}_i for which $z(\mathbf{x}) \leq z(\mathbf{x}_i) = 0, \forall \mathbf{x} \in \mathcal{N}_{\mathbf{x}_i}$. Finally, items (i) and (iv) let us conclude that $\forall \mathbf{x}_i \in \mathcal{X}$ maximize function (15) in a global sense. \square

Proof of Theorem 6 Continuity and completeness of the preference relation ensures that \succsim can be represented by a continuous utility function $u_{\succsim}(\mathbf{x})$ (Theorem 1). Consequently, the scoring function $f(\mathbf{x}) = -u_{\succsim}(\mathbf{x})$ is also continuous. Compactness of Ω guarantees the existence of a \succsim -maximum in Ω (see Proposition 1) and therefore Problem (3) admits a solution. Moreover, compactness of Ω and continuity of $f(\mathbf{x})$ are necessary hypotheses for Theorem 5.

Consider the sequence of iterates $\langle \mathbf{x}_i \rangle_{i \geq 1}$ produced by Algorithm 3. We define

- \mathcal{X}_{∞} as the set containing all the elements of $\langle \mathbf{x}_i \rangle_{i \geq 1}$,
- The subsequence of $\langle \mathbf{x}_i \rangle_{i \geq 1}$ containing only its first k entries as $\langle \mathbf{x}_i \rangle_{i=1}^k = \langle \mathbf{x}_1, \dots, \mathbf{x}_k \rangle$,
- \mathcal{X}_k as the collection of the points in $\langle \mathbf{x}_i \rangle_{i=1}^k$.

In practice, the first N entries of $\langle \mathbf{x}_i \rangle_{i \geq 1}$ constitute the initial set of samples \mathcal{X} (obtained by the LHD [22]), i.e. $\mathcal{X}_N = \mathcal{X}$, while the remaining ones are obtained by solving Problem (8). Note that $\hat{f}(\mathbf{x})$ is a continuous function since it is a linear combination of continuous functions (see for example the radial functions $\varphi(\cdot)$ in Section 3.1) and $z(\mathbf{x})$ is differentiable everywhere (Theorem 3), hence it is continuous as well. Therefore, $a(\mathbf{x})$ in (25) is continuous and, for the Extreme Value Theorem [1], Problem (8) always admits a solution. Thus, any sample \mathbf{x}_i obtained either by the experimental design or by solving Problem (8) is such that $\mathbf{x}_i \in \Omega$, making $\mathcal{X}_{\infty} \subseteq \Omega$.

Suppose now that $\Delta_{cycle} = \{0\}$, then, at each iteration, the new candidate sample \mathbf{x}_{k+1} ($k > N$) is found by solving:

$$\begin{aligned} \mathbf{x}_{k+1} &= \arg \min_{\mathbf{x}} \frac{z(\mathbf{x}) - z_{min}(\mathcal{X}_{aug})}{\Delta Z(\mathcal{X}_{aug})} \\ \text{s.t. } \mathbf{x} &\in \Omega, \end{aligned} \quad (36)$$

using the k samples at hand, which are contained in \mathcal{X}_k . Note that Problem (36) is equivalent to Problem (18) since scaling and shifting the objective function does not change its minimizer. From Proposition 2,

$$z(\mathbf{x}_i) = 0, \forall \mathbf{x}_i \in \mathcal{X}_k,$$

while, from (15),

$$z(\mathbf{x}) < 0, \forall \mathbf{x} \in \Omega \setminus \mathcal{X}_k.$$

Therefore, \mathbf{x}_{k+1} obtained by solving Problem (36) is $\mathbf{x}_{k+1} \notin \mathcal{X}_k$, which implies that, given any $\mathbf{x} \in \Omega$, $\mathbf{x} \in \mathcal{X}_k$ for $k \rightarrow \infty$. Since any point $\mathbf{x} \in \Omega$ will eventually be sampled by Problem (36), we can define a sequence

$$\langle \tilde{\mathbf{x}}_i \rangle_{i \geq 1} = \langle \tilde{\mathbf{x}}_1, \tilde{\mathbf{x}}_2, \dots \rangle$$

in \mathcal{X}_∞ as the concatenation of a sequence $\langle \mathbf{x}_i \rangle_{i=1}^k$ for k such that $\mathbf{x}_k = \mathbf{x}$ and a constant sequence of \mathbf{x} , i.e.

$$\langle \tilde{\mathbf{x}}_i \rangle_{i \geq 1} = \langle \mathbf{x}_1, \dots, \mathbf{x}_{k-1}, \mathbf{x}, \mathbf{x}, \dots \rangle.$$

By construction, $\langle \tilde{\mathbf{x}}_i \rangle_{i \geq 1}$ is such that

$$\lim_{i \rightarrow \infty} \tilde{\mathbf{x}}_i = \mathbf{x}. \quad (37)$$

We have proven that:

- $\mathcal{X}_\infty \subseteq \Omega$,
- Given any $\mathbf{x} \in \Omega$, there exists a sequence $\langle \tilde{\mathbf{x}}_i \rangle_{i \geq 1}$ in \mathcal{X}_∞ which satisfies (37).

Thus, we can conclude that \mathcal{X}_∞ is dense in Ω [19] and, consequently, so is the corresponding sequence of iterates $\langle \mathbf{x}_i \rangle_{i \geq 1}$. Finally, by Theorem 5, gMRS converges to the global minimizer of Problem (3). We can reach the same conclusion for any Δ_{cycle} that includes a zero entry. \square

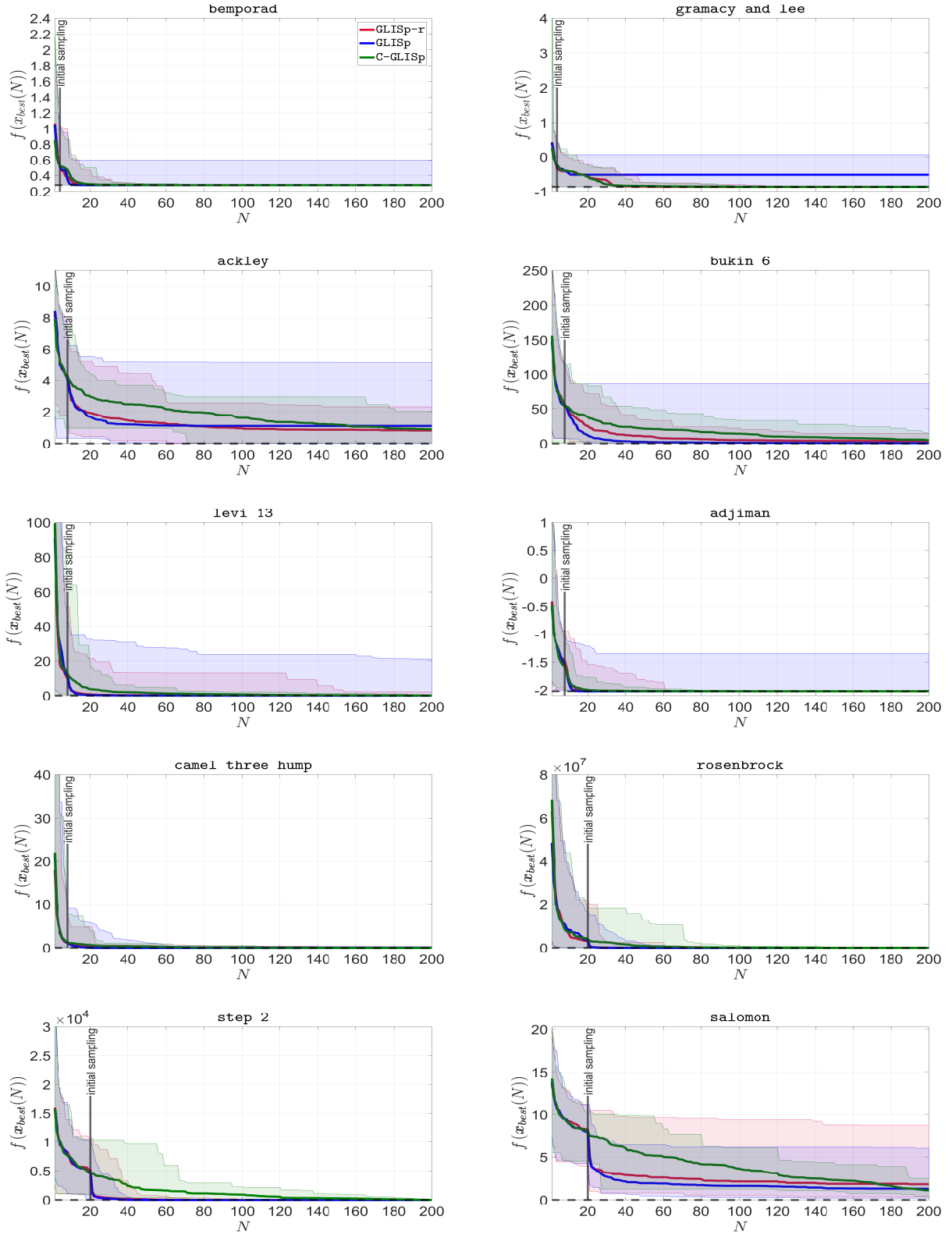


Figure 7: Performance comparison of preference-based optimization algorithms: GLISp [3] (blue) with $z(x)$ defined as in (15), C-GLISp [36] with $z(x)$ defined as in (28) (green) and GLISp-r (red). N is the number of samples and $f(x_{best}(N))$ is the function value achieved by the best sample when $|\mathcal{X}| = N$. The thick colored lines denote the median value, the shadowed areas remark the best and worst case instances, the dashed black line is the global minimum $f(x^*)$ and the black vertical line divides the initial sampling phase and the one based on the minimization of the acquisition function.

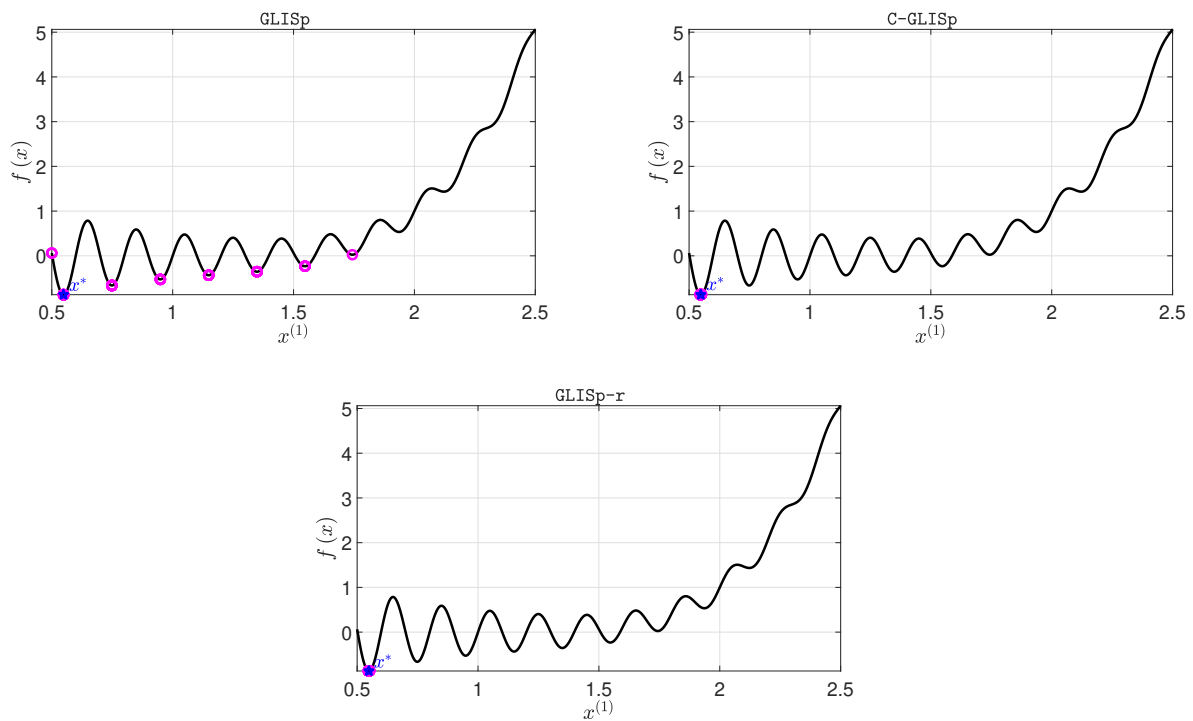


Figure 8: Best samples found by the preference-based optimization algorithms for function gramacy and lee [14] (black line). Each point in magenta represents $x_{best}(N_{max})$ for the corresponding simulation. The blue star is the global minimizer of Problem (3). Notice how, for some simulations, GLISp [3] gets stuck on one of the local minima, while C-GLISp [36] and GLISp-r converge to x^* more consistently.